

**Variational density functional perturbation theory for metals**Xavier Gonze<sup>1,\*</sup>, Samare Rostami<sup>1</sup> and Christian Tantardini<sup>2,3,†</sup><sup>1</sup>*European Theoretical Spectroscopy Facility, Institute of Condensed Matter and Nanosciences, Université catholique de Louvain, Chemin des étoiles 8, bte L07.03.01, B-1348 Louvain-la-Neuve, Belgium*<sup>2</sup>*Hylleraas center, Department of Chemistry, UiT The Arctic University of Norway, PO Box 6050 Langnes, N-9037 Tromsø, Norway*<sup>3</sup>*Department of Materials Science and Nanoengineering, Rice University, Houston, Texas 77005, USA*

(Received 30 October 2023; revised 25 December 2023; accepted 3 January 2024; published 30 January 2024)

Density functional perturbation theory (DFPT) is a well-established method to study responses of molecules and solids, especially responses to atomic displacements or to different perturbing fields (electric, magnetic). Like for density functional theory (DFT), the treatment of metals is delicate, due to the Fermi-Dirac (FD) statistics and electronic bands crossing the Fermi energy. At zero temperature, there is an abrupt transition from occupied states to unoccupied ones, usually addressed with smearing schemes. Also, at finite temperature, fractional occupations are present, and the occupation numbers may vary in response to the perturbation. In this paper, we establish the characteristics of DFPT stemming from the underlying variational principle, in the case of metals. After briefly reviewing variational DFT for metals, the convexity of the entropy function of the occupation number is analyzed, and at finite temperature, the benefit of resmearing the FD broadening with the Methfessel-Paxton one is highlighted. Then the variational expressions for the second-order derivative of the free energy are detailed, exposing the different possible gauge choices. The influence of the inaccuracies in the unperturbed wave functions from the prior DFT calculation is studied. The whole formalism is implemented in the ABINIT software package.

DOI: [10.1103/PhysRevB.109.014317](https://doi.org/10.1103/PhysRevB.109.014317)**I. INTRODUCTION**

Density functional perturbation theory (DFPT) has been implemented and used for decades for the study of responses of molecules, solids, and nanostructures to different types of perturbations, including atomic displacements, applied electric field or magnetic field, or cell parameter changes [1–10]. It proves a method of choice for the computation of phonon band structures [11], linear dielectric response [12], Born effective charges [13], thermal expansion [14,15], piezoelectricity [9], Raman tensors [16], electro-optic effect [17], electron-phonon [18,19] and phonon-phonon couplings [20,21], flexoelectricity [22], thermodynamical [15,23], and many other properties. The list of applications of DFPT continues to increase regularly.

Many basic concepts and theorems of DFPT have been established for a long time [1,2,4–7,24]. DFPT stems from the Taylor expansion of quantities present in density functional theory (DFT) when an external parameter is changed by a small amount. The abovementioned properties are directly connected to the (possibly high-order) derivatives of the energy with respect to such small parameters characterizing the strength of the perturbations. Since the first-order derivatives of the energy with respect to atomic displacement, electric field, magnetic fields, and cell parameter changes, respectively, are forces, electric dipole or electric polariza-

tion, magnetic dipole or magnetic polarization, and stress, their linear response to additional applied fields are linked to second-order derivatives of the energy.

It is well known that DFT is based on a variational principle: The energy is minimized with respect to trial Kohn-Sham wave functions. DFPT inherits also from this property of DFT a variational principle for the second-order derivative of the energy with respect to trial first-order wave functions [2]. While the linear-response formalism can be derived without making explicit usage of this variational property, the quantities computed numerically, determined using iterative solvers with some stopping criterion, are more accurate with the variational formulation than with alternative, possibly simpler, nonvariational formulations. Also, algorithms to determine the optimal first-order wave functions can benefit from the variational character of second-order energy. In addition, the variational principle is crucial for establishing higher-order DFPT, thanks to the so-called  $2n + 1$  theorem [4,20,24].

The specificities of the treatment of metals within DFPT have been established by de Gironcoli [3] based on the treatment of metals in DFT. At variance with the DFT theory for finite systems and insulators, in the DFT theory of metals, the occupation numbers, usually fractional, must be determined. The electronic entropy appears, and the internal energy is replaced by the free energy. Such varying occupation numbers are present when dealing with finite temperature but also appear in practice even at zero temperature to deal with the abrupt transition between occupied states and unoccupied states at the Fermi energy. Such a case is tackled using smearing schemes that allow one to reduce the numerical burden

\*xavier.gonze@uclouvain.be

†christiantantardini@gmail.com

of the integration of a discontinuous occupation function in the Brillouin zone. The most efficient high-order smearing schemes [25] have their own problems, as described by dos Santos and Marzari [26] since the occupation function of the energy becomes nonmonotonic.

For DFPT, de Gironcoli [3] described the specificities of linear responses due to varying occupation numbers and entropy and provided phonon band structures for Al, Pb, and Nb. However, he did not present a variational formulation of the second-order derivative of the free energy. This result is still lacking in the literature. However, it had been derived, implemented (at least in the ABINIT package) [27–29], and used for many studies of metals, e.g., for computing the phonon band structures of lead [30], bismuth [31,32], and polonium [33], all three with spin-orbit coupling, or the electronic transport properties of lithium [34], osmium, and osmium silicide [35], among others.

Motivated by the interest to fill this gap but also by some recent publications related to the response properties of metals by Cancès *et al.* [36] as well as improved treatment in high-order smearing schemes in DFT by dos Santos and Marzari [26], in this paper, we aim to lay down the variational treatment of DFPT for metals. The second-order derivative of the free energy is formulated as a variational functional of trial first-order wave functions and the trial first-order density matrix. The second-order entropy is present in the second-order free energy and depends on the first- and selected second-order changes of the occupation numbers, both derived from the first-order density matrix. Nonvariational expressions are also presented.

The invariance of DFT for metals with respect to unitary transformations inside the wave function space is more intricate than in the case of DFT for gapped systems at 0 K [4]. In the latter, a unitary transformation of wave functions inside the occupied space leaves the density, total energy, and Kohn-Sham potential invariant. In the case of metals, a unitary transformation of the wave functions must be accompanied by a simultaneous transformation of the (one-body) density matrix. The wave functions might not be eigenstates of the Hamiltonian, and the density matrix might not be diagonal. Still, such transformed trial wave functions and the trial density matrix correspond to the same free energy and hence minimize the free energy functional. This was developed by Marzari, Vanderbilt, and Payne (MVP) [37] in their variational formulation of DFT for metals, on which we will rely to derive the variational formulation of DFPT for metals.

As outlined for DFT above, in DFPT also, several sets of first-order wave functions (and first-order density matrix elements for the metal case) minimize the energy, related by some well-defined transformation rule. A choice among such possibilities is referred to fixing the gauge, and the invariance of the second-order free energy with respect to the gauge choice is called the gauge freedom. The gauge freedom in the DFPT of metals is more complicated than the one in the DFPT of gapped systems at 0 K, and this is described as well in this paper. The parallel and diagonal gauges are defined, extending to the metal case the well-known results obtained for gapped systems. However, more freedom is allowed, due to the added variability of the density matrix. This will be described as well, as different formulations might be of interest in different

contexts. A connection with the article by Cancès *et al.* [36] will be made.

Concerning smearing schemes, we first remark that the nonmonotonic behavior of the occupation number as a function of the energy not only induces problems at the level of the determination of the Fermi energy, as outlined recently by dos Santos and Marzari [26], but also makes the one-level entropy function of the occupation number multivalued and nonconvex. DFPT is also impacted, as the second-order free energy might not be an extremum because of the nonpositive definiteness of the contribution of the second-order entropy. When a finite temperature is considered, it is shown that the resmearing procedure [38] is a procedure in which possibly higher-order smearing might be used without sacrificing the monotonic behavior of the occupation function, provided the resmearing parameter is not too large. For the resmearing using the Methfessel-Paxton (MP) scheme [25], it is shown that a smearing parameter smaller or equal to twice the physical electronic temperature can be used. For such a range of parameters, the occupation function is monotonic, and the one-level entropy is univalued and convex.

Coming to applications, in addition to the results already available in the literature, the convergence of phonon frequencies of copper with respect to the wave vector grid and to smearing schemes is provided. For this case, one can distinguish two regimes: a first one, medium precision, in which the target numerical precision is requested at the level of the absolute value of phonon frequencies, and a second one, high precision, in which the target is the study of the temperature dependence of the phonon frequencies.

Finally, the impact of the precision requirement (or lack of precision) for the unperturbed wave functions on the precision of the second-order free energy is examined. Indeed, when dealing with metals, in practice, the preliminary DFT calculation of the density also includes wave functions with vanishing occupations. Depending on the stopping criterion, possibly the highest-energy ones might not be well converged, as they do not influence the density anyhow. Thus, the impact of lack of precision of such wave functions in DFT is negligible. By contrast, it is found that such a lack of numerical convergence might have an impact in the subsequent DFPT calculations, in agreement with the recent observation by Cancès *et al.* [36]. This impact is analyzed thanks to a simple three-level model. The error in the second-order free energy is found to be proportional to the norm of the residual of such wave functions. Cancès *et al.* [36] proposed a Schur complement technique to deal with such a problem. At variance, increasing the number of states in the underlying DFT calculation, then filtering less-converged states to start subsequent DFPT calculations solves the problem, if their occupation is really negligible.

The structure of this paper is as follows. After this introduction, Sec. II deals with variational DFT for metals: The MVP [37] variational DFT for metals is reviewed, some considerations on the space of potentially occupied wave functions are introduced, and then smearing schemes are detailed. In the latter, it is shown that resmearing [38] the Fermi-Dirac (FD) distribution with the MP smearing [25] at finite temperature does not break the monotonic behavior of the occupation function, for a range of resmearing parameter. Related to Sec. II,

Sec. S1 in the Supplemental Material [39] fixes notation problems and typos present in Ref. [38].

In Sec. III, the variational second-order free energy within DFPT that includes the treatment of the second-order entropy is presented. The gradient of the second-order free energy is written and linked with the de Gironcoli [3] linear-response DFPT approach for metals. In the Supplemental Material [39], Sec. S2 gives a detailed derivation of the variational second-order free energy, while Secs. S3 and S4 give some technical details to obtain the gradients, also related to the nonhermiticity freedom for the first-order off-diagonal density matrix elements.

Section IV focuses on the choice of gauge. The gauge freedom is first presented, followed by the definition and properties of the parallel gauge as well as the definition and properties of the diagonal gauge. The section finishes with the complete suppression of first-order occupation matrix elements. In the Supplemental Material [39], the covariance of first-order wave functions and first-order density matrix elements is presented in Sec. S5. Then the derivation of the first-order density expression with modified first-order wave functions is explained in Sec. S6, and finally, nonvariational expressions are written, for the case of the parallel gauge, in Sec. S7.

While the previous sections neglected the Bloch characteristics of the first-order wave functions and energies as well as the presence of a Brillouin zone, Sec. V upgrades such results for explicitly periodic systems.

Section VI presents the study of some phonon frequencies of copper, especially focusing on the wave vector grid sampling and its interplay with the smearing parameter. The medium- and high-precision regimes are distinguished. In the Supplemental Material [39], Sec. S8 provides additional figures.

The influence of underconverged unoccupied states on the second-order free energy is quantified and analyzed using a simple model in Sec. VII, with details of the mathematical treatment given in the Supplemental Material [39], Sec. S9.

Section VIII summarizes the results.

## II. VARIATIONAL DFT FOR METALS

In this section, first, the variational approach to DFT of metals [37] is reviewed, with notations that will then be used to treat the DFPT case. The need to define a space of potentially occupied wave functions is highlighted. Smearing schemes are the focus of the last part of this section on DFT. The monotonic behavior of the occupation function is linked to the convexity and single-valuedness of the entropy function of the occupation number.

### A. Variational formulation of DFT with varying occupation numbers at finite temperature

MVP [37] introduced a variational free energy for the DFT with varying occupation numbers at finite temperature, especially relevant to treat metals. This approach will also be a basis for variational DFPT. For simplicity, the formalism is presented for nonspin-polarized systems ( $n_s = 2$  accounts for the spin degeneracy). Generalization to spin-polarized

systems, including the noncollinear case, is trivial. In this section as well as Secs. III and IV, one considers finite systems (with  $N$  being the total number of electrons). Periodic systems are treated in Sec. V. Atomic (Hartree) units are used throughout.

The MVP electronic free energy  $F[T; \{\psi_i\}, \{\rho_{ij}\}]$ , for a given temperature  $T$ , is a functional of the (trial) wave functions  $\{\psi_i\}$  that form an orthonormal basis set and of the (trial) matrix representation  $\{\rho_{ij}\}$  of the one-particle density matrix operator  $\hat{\rho}$  in this orthonormal set. Explicitly:

$$F[T; \{\psi_i\}, \{\rho_{ij}\}] = n_s \sum_{ij} \rho_{ji} \langle \psi_i | \hat{K} + \hat{v}_{\text{ext}} | \psi_j \rangle + E_{\text{Hxc}}[\rho] - TS[\{\rho_{ij}\}]. \quad (1)$$

In this expression, the sums over  $i$  and  $j$  extend to infinity,  $\hat{K}$  is the kinetic energy operator,  $\hat{v}_{\text{ext}}$  is the external potential (e.g., created by the nuclei as well as any other additional external potential), and  $E_{\text{Hxc}}$  is the DFT Hartree and exchange-correlation energy functional of the density  $\rho(\mathbf{r})$ , which is defined as

$$\rho(\mathbf{r}) = n_s \sum_{ij} \rho_{ji} \psi_i^*(\mathbf{r}) \psi_j(\mathbf{r}). \quad (2)$$

The one-particle density matrix is Hermitian, with all its eigenvalues  $f_\gamma$ —occupation numbers of the corresponding state—being between 0 and 1 for the FD entropy (see later for the behavior of occupation numbers with high-order smearing schemes). Here,  $S[\{\rho_{ij}\}]$  is the entropy, considered as a functional of the density matrix elements. Explicitly,

$$S[\{\rho_{ij}\}] = n_s \sum_{\gamma} k s(f_\gamma) = n_s \text{Tr}[k s(\hat{\rho})], \quad (3)$$

where  $s(f)$ , the one-level entropy function (adimensional), is to be specified, and  $k$  is Boltzmann's constant. The usual physical situation corresponds to the FD entropy function  $s_{\text{FD}}(f)$ , given by

$$s_{\text{FD}}(f) = -[f \ln(f) + (1 - f) \ln(1 - f)]. \quad (4)$$

Smearing techniques, introduced for numerical reasons, will modify such an entropy function. In what follows, equations are presented in terms of a generic  $s(f)$  function, with examples using the FD entropy function. The formulas for other entropy functions are presented in Sec. II C.

The trace of the occupation matrix is constrained to  $N$ , the number of electrons, possibly considering the spin degeneracy:

$$n_s \sum_i \rho_{ii} = n_s \sum_{\gamma} f_{\gamma} = N. \quad (5)$$

Following MVP [37], one defines the Hamiltonian matrix, with elements:

$$H_{ij}[\rho] = \langle \psi_i | \hat{K} + \hat{v}_{\text{ext}} + \hat{v}_{\text{Hxc}}[\rho] | \psi_j \rangle, \quad (6)$$

where  $\hat{v}_{\text{Hxc}}[\rho]$  is a local operator, with

$$v_{\text{Hxc}}[\rho](\mathbf{r}) = \frac{\delta E_{\text{Hxc}}[\rho]}{\delta \rho(\mathbf{r})}. \quad (7)$$

MVP introduced the Lagrange multiplier  $\mu$  (identified to the chemical potential) that enforces the constraint Eq. (5). It is such that

$$H_{ij}[\rho] - kT[s'(\hat{\rho})]_{ij} = \mu\delta_{ij}, \quad (8)$$

where the notation  $[s'(\hat{\rho})]_{ij}$  is used in place of  $d(\text{tr}[s(\hat{\rho})])/d\rho_{ji}$ . MVP also obtained that, at the minimum, the Hamiltonian and occupation matrices can be simultaneously diagonalized.

Working with the diagonal Hamiltonian and occupation matrices is convenient, but one is free to avoid diagonalizing them, the so-called gauge freedom that MVP exploited indeed. Arbitrary unitary transformations between the wave functions can be accompanied by adequate unitary transformation of the occupation matrix, such that the density [Eq. (2)], the entropy [Eq. (3)], and the free energy [Eq. (1)] are invariant.

If the wave functions are chosen to diagonalize both Hamiltonian and density matrices, one has

$$H_{ij}[\rho] = \epsilon_i\delta_{ij}, \quad (9)$$

and

$$\epsilon_i - kT s'(f_i) = \mu. \quad (10)$$

For the FD entropy,

$$s'_{\text{FD}}(f) = \frac{ds_{\text{FD}}}{df} = \ln\left(\frac{1}{f} - 1\right). \quad (11)$$

Equation 10 can be inverted to deliver the occupation number as a function of the eigenenergy:

$$f_i = [s']^{-1}\left(\frac{\epsilon_i - \mu}{kT}\right), \quad (12)$$

where the notation  $[s']^{-1}$  is for the reciprocal of the  $s'$  function.

For the FD entropy function defined in Eq. (4), Eq. (12) delivers the usual FD occupations, where

$$f_i = f_{\text{FD}}\left(\frac{\mu - \epsilon_i}{kT}\right), \quad (13)$$

$$f_{\text{FD}}(x) = [\exp(-x) + 1]^{-1}. \quad (14)$$

Note that, for consistency with the usual definitions for smearing schemes, we choose the  $f_{\text{FD}}(x)$  function to monotonically increase from 0 to 1. Then Eq. (13) is such that, for high-energy states (large  $\epsilon_i$ ), the occupation number tends rapidly to zero exponentially.

In what follows, the choice to diagonalize the Hamiltonian (together with the occupation matrix) will be referred to as the diagonal gauge. In the diagonal gauge,

$$\hat{H}|\psi_i\rangle = (\hat{K} + \hat{v}_{\text{ext}} + \hat{v}_{\text{Hxc}}[\rho])|\psi_i\rangle = \epsilon_i|\psi_i\rangle. \quad (15)$$

For the derivation of DFPT equations, done later, this variational formulation of DFT for metals at finite temperature is reformulated as an unconstrained minimization, based on

Lagrange multipliers, as follows. The free energy is augmented with the Lagrange contributions from both types of constraints, namely,

$$\begin{aligned} F^+[T; \{\psi_i\}, \{\rho_{ij}\}] &= F[T; \{\psi_i\}, \{\rho_{ij}\}] \\ &- \sum_{ij} \Lambda_{ji} n_s (\langle \psi_i | \psi_j \rangle - \delta_{ij}) \\ &- \mu \left( n_s \sum_i \rho_{ii} - N \right). \end{aligned} \quad (16)$$

The optimal electronic free energy  $F_{\text{el}}(T)$  is obtained by minimizing such augmented free energy:

$$F_{\text{el}}[T] = \min_{\{\psi_i\}, \{\rho_{ij}\}} F^+[T; \{\psi_i\}, \{\rho_{ij}\}], \quad (17)$$

without specific constraints on  $\{\psi_i\}, \{\rho_{ij}\}$  during the minimization but where the Lagrange multipliers  $\Lambda_{ji}$  and  $\mu$  are chosen to enforce them afterwards. In this formulation as well, unitary transforms between the wave functions and occupation matrix leave the density, entropy, and free energy invariant. One can check that, at the minimum,

$$\Lambda_{ki} = \sum_j H_{kj} \rho_{ji}. \quad (18)$$

In the diagonal gauge, this becomes

$$\Lambda_{ji} = \epsilon_i \delta_{ji} \rho_{ii}. \quad (19)$$

## B. The space of potentially occupied wave functions

In practice, first-principles calculations for metals at finite temperature (or finite smearing) only explicitly treat a finite number of eigenstates, among which some are (nearly) fully occupied, some have intermediate occupation numbers, and some have vanishing occupation numbers. Occupation numbers of the states outside of this space of potentially occupied states are so small that they can be set to zero and ignored. Thus, there is an active space of potentially occupied wave functions. This space plays the same role as the occupied state space for the first-principles treatment of semiconductors.

This approach might not be practical when the temperature is quite large, yielding a large number of wave functions in the active space. However, even a temperature as high as 6000 K (corresponding to  $\sim 0.5$  eV, which is beyond melting of all known materials at ordinary pressure) does not induce an unreasonable increase of the number of states compared with the number of bands strictly needed at 0 K.

The number of potentially occupied wave functions,  $p_{\text{occ}}$ , is defined at the start of the computation. It must sufficiently exceed the number of electrons  $N$  for the highest states in this space to have vanishing occupations. Thus, instead of minimizing Eq. (16) with the definition in Eq. (1), which implicitly supposes that the set of  $\{\psi_i\}$  spans the whole Hilbert space, the functional to be considered is defined in terms of a finite number of orthonormal functions and the corresponding finite occupation matrix elements, with  $i$  and  $j$  running from

1 to  $pocc$ . This gives the following modified definition:

$$\begin{aligned}
 F^+[T, \{\psi_i\}, \{\rho_{ij}\}] &= n_s \sum_{ij}^{\text{pocc}} \rho_{ji} h_{ij} + E_{\text{Hxc}}[\rho] - kT n_s \sum_{\gamma} s(f_{\gamma}) \\
 &\quad - \sum_{ij}^{\text{pocc}} \Lambda_{ji} n_s (\langle \psi_i | \psi_j \rangle - \delta_{ij}) - \mu \left[ \left( \sum_i^{\text{pocc}} n_s \rho_{ii} \right) - N \right].
 \end{aligned} \tag{20}$$

The orthonormalization constraint only applies between the functions belonging to the potentially occupied wave functions. The notation  $S_{\text{pocc}}$  will later denote that space of functions.

### C. Smearing schemes

Smearing schemes aim to decrease the numerical effort needed to deal with rapidly varying occupation numbers when the Brillouin zone of metals is sampled. They allow one to rely on fewer wave vectors to obtain the same numerical precision as without smearing. The difficulty to reach numerical convergence is especially acute for a vanishing temperature since the occupation of levels discontinuously changes from 1 to 0 at the Fermi level. Generally speaking, the occupation of an energy level is defined through an occupation function  $f(x)$  whose argument is the difference between the Fermi energy and the energy of the level, rescaled by either  $kT$ , for the FD case, or by a smearing energy  $\sigma$ , for pure numerical smearing schemes. The occupation function  $f(x)$  vanishes for infinitely negative  $x$  and tends to 1 for infinitely positive  $x$ .

As mentioned in Refs. [25,26], all such occupation functions can be generated from an associated smearing function  $\tilde{\delta}(\varepsilon)$ , which is normalized to 1. The related occupation function is

$$f(x) = \int_{-\infty}^x \tilde{\delta}(\varepsilon) d\varepsilon, \tag{21}$$

where  $x = \frac{\mu - \varepsilon}{\sigma}$ . Note that  $x$  is adimensional as well as the integrand  $\varepsilon$ , while  $\varepsilon$ ,  $\mu$ ,  $\sigma$ , and  $kT$  have the dimension of energy. Here,  $x$  and  $\varepsilon$  are rescaled energies without dimensions. For the FD case, the smearing function is

$$\tilde{\delta}_{\text{FD}}(x) = \frac{1}{[\exp(x) + 1][\exp(-x) + 1]}. \tag{22}$$

The occupation function deduced from this smearing function is given by Eqs. (13) and (14), as expected.

To obtain the entropy  $s(f)$  as a function of the occupation, one first defines the entropy  $\tilde{s}(x)$  as a function of the adimensional  $x$ :

$$\tilde{s}(x) = - \int_{-\infty}^x \varepsilon \tilde{\delta}(\varepsilon) d\varepsilon. \tag{23}$$

Note the slight change of notation for the entropy function of the rescaled energy  $\tilde{s}$  with respect to the one in Ref. [26],  $s$  for the same quantity. Indeed, the notation  $s$  is already used in the present context for the entropy as a function of  $f$ , see Eq. (3). The latter had not been examined in Ref. [26].

Such a function  $s(f)$  is deduced from Eq. (23) by using the reciprocal of the function  $f$  defined in Eq. (21), denoted  $[f]^{-1}$  so that

$$s(f) = \tilde{s}\{[f]^{-1}(f)\}. \tag{24}$$

Indeed, with definitions Eqs. (21) and (23) and the same definition of  $x$  as in the text before Eq. (21), the relation Eq. (12), which links the occupation number to the energy through the derivative of the entropy as a function of the occupation number, is fulfilled. Note, however, that  $s(f)$  might be a multivalued function in the case where the  $f(x)$  function is not monotonically decreasing. This is encountered for advanced smearing schemes. Also, the one-level contribution to the free energy  $-Ts(f)$  might not be convex.

For the FD case, the corresponding  $-kT s_{\text{FD}}(f)$ , Eq. (4), is univalued and convex.

Beyond the FD case, the Gaussian (G) and MP smearing functions are often encountered. We will not analyze so-called cold smearings [40] which, for the purpose of the present analysis, exhibit the same problematic feature as the MP smearing, namely, the nonmonotonicity of the occupation function.

For the G case, the smearing function is

$$\tilde{\delta}_{\text{G}}(x) = \frac{1}{\sqrt{\pi}} \exp(-x^2). \tag{25}$$

The occupation function  $f_{\text{G}}(x)$  is  $1 + \text{erf}(x)/2$ . Its reciprocal cannot be expressed easily. The entropy function of  $x$  is half the broadening function:

$$\tilde{s}_{\text{G}}(x) = \frac{1}{2\sqrt{\pi}} \exp(-x^2). \tag{26}$$

This entropy function of the occupation is univalued.

For the MP broadening,

$$\tilde{\delta}_{\text{MP}}(x) = \frac{1}{\sqrt{\pi}} \left( \frac{3}{2} - x^2 \right) \exp(-x^2), \tag{27}$$

$f_{\text{MP}}(x)$  can be  $>1$  and  $<0$  and is not easily expressed. It is not monotonically increasing; hence, the  $s_{\text{MP}}(f)$  function is multivalued. The corresponding entropy function of the scaled energy is

$$\tilde{s}_{\text{MP}}(x) = \frac{1}{2\sqrt{\pi}} \left( \frac{1}{2} - x^2 \right) \exp(-x^2). \tag{28}$$

By convention, for the G and MP scheme, one replaces  $kT$  by the smearing parameter  $\sigma$  in the definition of the individual occupations in terms of the distribution function, Eq. (13). As mentioned earlier, the goal of the G and MP smearings is to provide the  $T = 0$  properties of metals with less numerical effort than with the sudden change of the occupation from 1 to 0 at the Fermi energy, albeit with some loss of precision, nevertheless under control. The advantage of the MP smearing function comes from vanishing low-order Taylor terms up to and including the third order with respect to the smearing parameter  $\sigma$  in the expansion of the correction to the free energy due to the smearing. In the G smearing, the second order does not vanish, while it vanishes for MP and cold smearing. However, as mentioned above, the MP occupation function becomes nonmonotonic.

At finite temperatures, a smearing methodology can also help. The so-called resmearing scheme has been introduced

to obtain physical finite-temperature quantities with decreased numerical effort [38,41]. The resmeared delta function  $\tilde{\delta}_{\text{rsm}}$  is defined as

$$\tilde{\delta}_{\text{rsm}}(y, R) = \int \tilde{\delta}_{\text{FD}}(y - Rz) \tilde{\delta}_2(z) dz, \quad (29)$$

where  $R = \frac{\sigma}{kT}$  is the ratio between the smearing parameter and the physical electronic temperature, and  $\delta_2$  is the broadening function (either the G broadening or the MP broadening in this paper) that is convoluted with the FD broadening function  $\tilde{\delta}_{\text{FD}}$ . While the broadening function  $\delta_2$  might indeed be such a generic function, in the remainder of this paper, we will focus on the case  $\delta_2 = \delta_{\text{MP}}$ .

The actual broadening function corresponding to some physical electronic temperature  $T$ , denoted as the total broadening in Refs. [38,41], is obtained as

$$\tilde{\delta}_{\text{tot}}(\mu - \epsilon, kT, \sigma) = \frac{1}{kT} \tilde{\delta}_{\text{rsm}}\left(\frac{\mu - \epsilon}{kT}, \frac{\sigma}{kT}\right), \quad (30)$$

where the explicit dependence of such a function on three arguments having the dimension of an energy has been made clear.

While preparing this paper, it became clear that the notation in Ref. [38], to which one of us contributed, was fuzzy. Also, several typos were present. To bypass such problems, Sec. S1 in the Supplemental Material [39] contains a mathematically rigorous rewriting of the key equations found in the original reference.

Depending on the ratio  $R$ , the total broadening resembles the original FD broadening (small  $R$ ) or the other broadening function  $\tilde{\delta}_2$  (large  $R$ ), although in the latter case, its argument is rescaled by  $R$ , and its value is inversely rescaled by  $R$ , to keep the integral unity.

For the specific resmearing of the FD broadening with MP broadening function, the value  $R = 2$  is critical since it is the largest  $R$  value for which the total broadening is positive for the entire range of its argument, as will be shown later. For this reason, the resmeared function with  $R = 2$  will be illustrated: In the forthcoming figures, results are presented with a smearing parameter  $\sigma$  twice as big as the energy corresponding to the physical electronic temperature  $kT$ . Note that the authors of Ref. [26] used  $R$  of  $\sim 2.565$  in comparing the FD and G cases. On the one hand, they were interested in working with the FD and G functions, while we are interested in the FD and MP functions, and on the other hand, they based their study on another criterion (the similarity between the G and FD occupation function). In practice, the resmearing parameter  $\sigma$  is, however, taken to be a constant, irrespective of the physical electronic temperature.

Figure 1(a) presents the different broadening functions mentioned above (with  $R = 2$  and  $\delta_2 = \delta_{\text{MP}}$  for  $\tilde{\delta}_{\text{rsm}}$ ). All functions, except MP, are positive, going smoothly from 0 to their maximum then back to 0. Only the MP broadening exhibits negative values for some range of its argument. The asymptotic behavior of  $\tilde{\delta}_{\text{rsm}}$  is analyzed in Sec. S1 in the Supplemental Material [39]. It is shown there that the exponentially decreasing tail of  $\tilde{\delta}_{\text{rsm}}$  changes sign at  $R = 2$ .

Similarly, Fig. 1(b) presents the different associated occupation functions, with the characteristic monotonically increasing behavior, except for the MP scheme, and Fig. 1(c)

presents the different one-level entropy functions  $\tilde{s}(x)$ , all positive everywhere except the MP one. In the context of the variational DFT (or DFPT), the shape of the entropy function with the occupation as argument  $s(f)$  is crucial. Indeed, it enters the free energy to be minimized through the  $-kTs(f)$  contribution of each one-electron level. Nonconvexity of this term might induce nonconvexity of the global free-energy functional.

The positive monotonic behavior of  $\frac{\partial f}{\partial x}$  is directly linked to the convexity of the  $-kTs(f)$  function. Indeed, using the chain rule followed by Eqs. (21) and (23), one finds

$$\frac{\partial s}{\partial f} = \frac{\partial \tilde{s}}{\partial x} \frac{\partial x}{\partial f} = -x \tilde{\delta}(x) [\tilde{\delta}(x)]^{-1} = -x. \quad (31)$$

This equation is derived with respect to  $f$  to give

$$\frac{\partial^2 s}{\partial f^2} = -\frac{\partial x}{\partial f} = -\left(\frac{\partial f}{\partial x}\right)^{-1}. \quad (32)$$

Thus, if  $\frac{\partial f}{\partial x} \geq 0$  everywhere, then also everywhere

$$\frac{\partial^2 s}{\partial f^2} \leq 0, \quad (33)$$

and  $-kTs(f)$  is convex. Here,  $\frac{\partial f}{\partial x} \geq 0$  everywhere is also the criterion to avoid multiple chemical potentials, as described in Ref. [26]. This criterion is violated by the MP scheme but fulfilled in the other schemes.

The  $s(f)$  function is represented in Fig. 1(d) for the different smearing schemes. The MP one is particularly interesting. Its domain of definition extends beyond the 0–1 range, and outside of this range, the function is multivalued, with two branches. This multivalued function has characteristic singularities at the smallest values that it can reach, where two branches merge with a common tangent. This happens at the critical rescaled energy  $x^*$  at which the broadening MP function vanishes,  $x^* = \pm\sqrt{\frac{3}{2}}$ . Indeed, at that value, both  $f_{\text{MP}}(x)$  and  $\tilde{s}_{\text{MP}}(x)$  reach an extremum. Their curvature is identical on the left and right of  $x^*$ , which explains the common tangent.

### III. SECOND-ORDER FREE ENERGY FOR METALS

#### A. Variational formulation of DFPT for metals

Reference [24] describes a general framework for the perturbation theory of variational principles, including the case of constraints. In Ref. [4], such a framework is applied to DFT in the case of discretized levels and fixed occupation numbers at 0 K. We follow the variational framework of Ref. [24], including its notations, and generalize Ref. [4] to varying metallic occupations. The details of the derivation are presented in Sec. S2 in the Supplemental Material [39].

For the unperturbed wave functions and occupation matrix, one works in the diagonal gauge: The starting wave functions  $|\psi_i^{(0)}\rangle$ , belonging to  $S_{\text{pocc}}$ , fulfill Eq. (15), and the unperturbed occupation numbers are obtained from Eq. (12)—or its equivalent for smearing schemes other than FD. Due to Eq. (15), all off-diagonal elements of the unperturbed density matrix vanish.

The augmented variational second-order free energy, a functional of the first-order wave functions and first-order

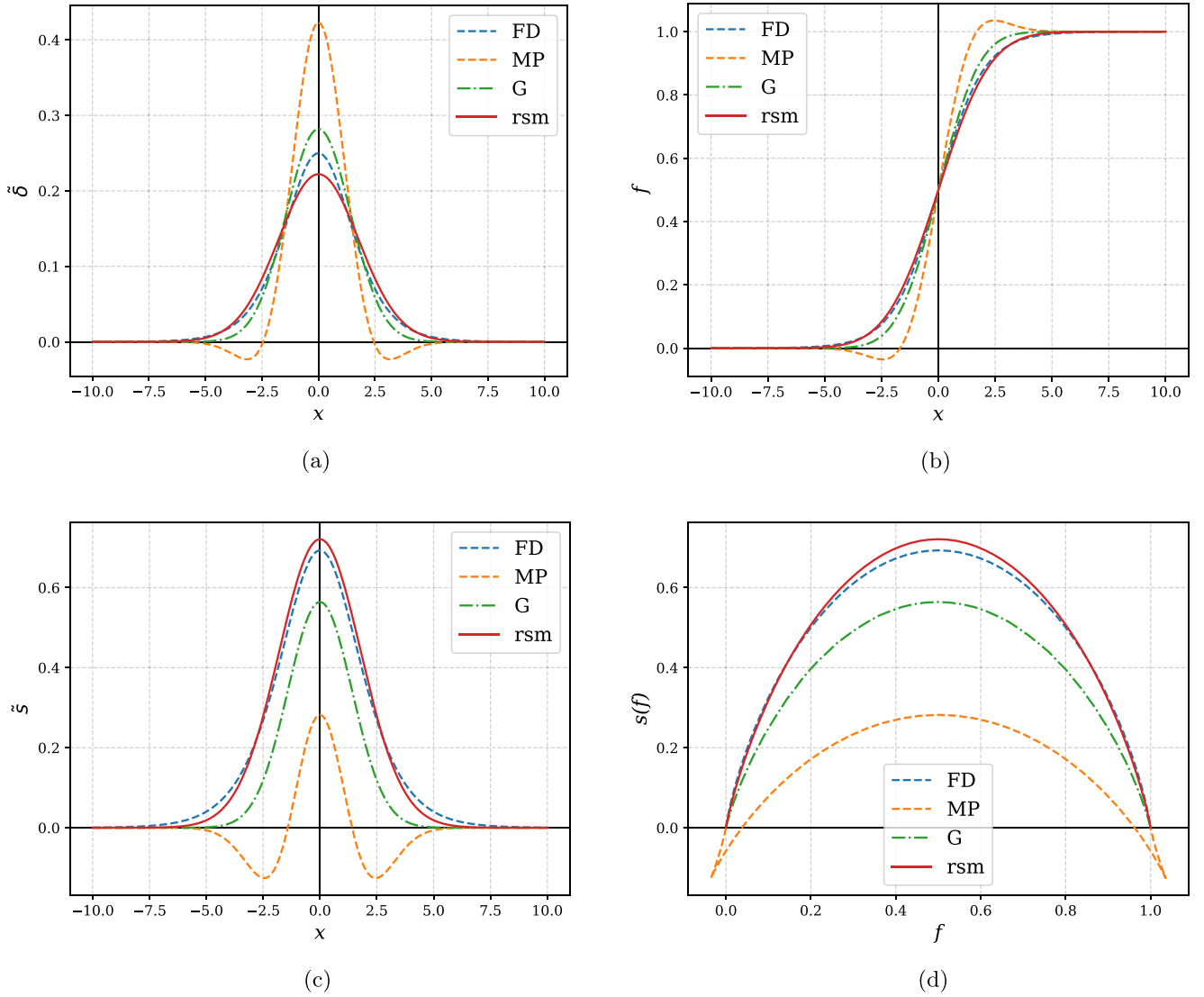


FIG. 1. Comparative representation of the broadening function, occupation function, and entropy functions ( $\tilde{s}$  and  $s$ ) in the Fermi-Dirac (FD), Methfessel-Paxton (MP), Gaussian (G), and resmeared cases. The last three are displayed with rescaling factor  $R = 2$ . Also,  $\delta_2 = \delta_{\text{MP}}$  for the resmeared case. (a) Comparative representation of the Fermi-Dirac broadening function  $\tilde{\delta}_{\text{FD}}(x)$  with the rescaled Methfessel-Paxton one  $R\tilde{\delta}_{\text{MP}}(x/R)$ , the rescaled Gaussian one  $R\tilde{\delta}_{\text{G}}(x/R)$ , and the rescaled smearing one  $R\tilde{\delta}_{\text{rsm}}(x/R, R)$ , with  $R = 2$ , see text, (b) Comparative representation of various occupation functions  $\tilde{\delta}_{\text{FD}}(x)$ ,  $f_{\text{MP}}(x/R)$ ,  $f_{\text{G}}(x/R)$ , and  $f_{\text{rsm}}(x/R, R)$ , with  $R = 2$ , see text. (c) Comparative representation of various entropy functions  $\tilde{s}_{\text{FD}}(x)$ ,  $\tilde{s}_{\text{MP}}(x/R)$ ,  $\tilde{s}_{\text{G}}(x/R)$  and  $\tilde{s}_{\text{rsm}}(x/R, R)$ , with  $R = 2$ , see text, and (d) Comparative analysis of various entropy functions  $s(f)$  of the occupation  $f$ .

density matrix elements, including Lagrange multipliers terms, is obtained as

$$\begin{aligned}
 F^{+(2)}[T, \{\psi_i^{(1)}\}, \{\rho_{ij}^{(1)}\}] &= n_s \sum_i^{\text{pocc}} f_i^{(0)} F_i^{(2)}[\psi_i^{(1)}] + n_s \sum_{ij}^{\text{pocc}} \rho_{ji}^{(1)} F_{ij}^{(1)}[\psi_i^{(1)}] + \frac{1}{2} \iint K_{\text{Hxc}}(\mathbf{r}, \mathbf{r}') \rho^{(1)}(\mathbf{r}) \rho^{(1)}(\mathbf{r}') d\mathbf{r} d\mathbf{r}' \\
 &\quad - TS^{(2)}[T; \{\rho_{ij}^{(1)}\}] - n_s \sum_{ij}^{\text{pocc}} \Lambda_{ji}^{(1)} [\langle \psi_i^{(1)} | \psi_j^{(0)} \rangle + \langle \psi_i^{(0)} | \psi_j^{(1)} \rangle] - n_s \mu^{(1)} \sum_i^{\text{pocc}} \rho_{ii}^{(1)}, \quad (34)
 \end{aligned}$$

with the shorthand notations

$$\begin{aligned}
 F_i^{(2)}[\psi_i^{(1)}] &= \langle \psi_i^{(1)} | \hat{H}^{(0)} - \epsilon_i^{(0)} | \psi_i^{(1)} \rangle + \langle \psi_i^{(0)} | \hat{v}_{\text{ext}}^{(2)} | \psi_i^{(0)} \rangle \\
 &\quad + [\langle \psi_i^{(1)} | \hat{v}_{\text{ext}}^{(1)} | \psi_i^{(0)} \rangle + \text{c.c.}], \quad (35)
 \end{aligned}$$

and

$$\begin{aligned}
 F_{ij}^{(1)}[\psi_i^{(1)}] &= \langle \psi_i^{(0)} | \hat{v}_{\text{ext}}^{(1)} | \psi_j^{(0)} \rangle + \langle \psi_i^{(1)} | \hat{H}^{(0)} | \psi_j^{(0)} \rangle \\
 &\quad + \langle \psi_i^{(0)} | \hat{H}^{(0)} | \psi_j^{(1)} \rangle. \quad (36)
 \end{aligned}$$

The dependence of this second-order free energy  $F^{+(2)}$  on the zeroth-order quantities  $\{|\psi_i^{(0)}\rangle\}$  and  $\{f_i^{(0)}\}$  is not mentioned explicitly, for sake of compactness. Similarly, the dependence of the second-order entropy  $S^{(2)}$  on  $\{f_i^{(0)}\}$  is not mentioned. This choice is made because the unperturbed system is considered known, and one is focusing on the effect of perturbations on the system. In Sec. VII, we will study the effect of underconverged  $\{|\psi_i^{(0)}\rangle\}$ .

The temperature is explicitly mentioned as an argument of  $F^{+(2)}$  and  $S^{(2)}$ . They indeed depend on it directly. Moreover, note that a change of  $T$  also affects  $|\psi_i^{(0)}\rangle$  and  $\{f_i^{(0)}\}$  and thus, indirectly,  $F^{+(2)}$  and  $S^{(2)}$ .

The Hartree and exchange-correlation kernel is defined as

$$K_{\text{Hxc}}[\rho](\mathbf{r}, \mathbf{r}') = \frac{\delta^2 E_{\text{Hxc}}[\rho]}{\delta\rho(\mathbf{r})\delta\rho(\mathbf{r}')}. \quad (37)$$

The first-order density is computed from

$$\begin{aligned} \rho^{(1)}(\mathbf{r}) &= n_s \sum_i^{\text{pocc}} f_i^{(0)} [\psi_i^{(1)*}(\mathbf{r})\psi_i^{(0)}(\mathbf{r}) + \psi_i^{(0)*}(\mathbf{r})\psi_i^{(1)}(\mathbf{r})] \\ &+ n_s \sum_{ij}^{\text{pocc}} \rho_{ji}^{(1)} \psi_i^{(0)*}(\mathbf{r})\psi_j^{(0)}(\mathbf{r}). \end{aligned} \quad (38)$$

As in the case of the unperturbed situation, the minimization of the augmented second-order free energy delivers the optimal electronic second-order free energy:

$$F_{\text{el}}^{(2)}[T] = \min_{\{\psi_i^{(1)}\}, \{\rho_{ij}^{(1)}\}} F^{+(2)}[T; \{\psi_i^{(1)}\}, \{\rho_{ij}^{(1)}\}]. \quad (39)$$

The Lagrange parameters  $\Lambda_{ji}^{(1)}$  and  $\mu^{(1)}$  in Eq. (34) must be tuned, after minimization, so that the constraints

$$\langle \psi_i^{(1)} | \psi_j^{(0)} \rangle + \langle \psi_i^{(0)} | \psi_j^{(1)} \rangle = 0, \quad (40)$$

for  $i$  and  $j$  in  $S_{\text{pocc}}$ , and

$$\sum_i^{\text{pocc}} \rho_{ii}^{(1)} = 0 \quad (41)$$

are enforced.

The second-order entropy term, evaluated with zeroth- and first-order elements of the density matrix (no second-order elements, see Ref. [4,24]) needs to be worked out carefully. Indeed, although none of the second-order elements of the density matrix should be considered (following Ref. [24]), the eigenvalues of the density matrix will be modified up to second order from first-order variations of the density matrix, and this will have an effect on the evaluation of the trace present in the second-order entropy term. From Eq. (3),

$$\begin{aligned} (S[\{\rho_{ij}^{(1)}\}])^{(2)} &= n_s \sum_{\gamma} k [s(f_{\gamma})]^{(2)} \\ &= n_s \sum_{\gamma} k \left\{ s'[f_{\gamma}^{(0)}] f_{\gamma}^{(2)} + s''[f_{\gamma}^{(0)}] \frac{[f_{\gamma}^{(1)}]^2}{2} \right\}. \end{aligned} \quad (42)$$

In the FD case, the first-order derivative of  $s$  with respect to its argument is given by Eq. (11), while the second-order derivative is

$$s''_{\text{FD}}(f) = \frac{d^2 s_{\text{FD}}}{df^2} = -\frac{1}{(1-f)f}, \quad (43)$$

a function that is negative for all values of  $f$  between 0 and 1, with negative curvature in this range, and that diverges at both 0 and 1. Considering the  $-kT$  prefactor of the second-order entropy in the augmented second-order free energy, Eq. (34), the  $s''$  term gives a positive contribution to that second-order free energy. The derivatives of occupation matrix eigenvalues  $f_{\gamma}^{(1)}$  and  $f_{\gamma}^{(2)}$  are to be computed from  $f_i^{(0)}$  and  $\rho_{ij}^{(1)}$ , excluding any higher-order contribution from the occupation matrix, in line with the general DFPT formalism [4,24]. The eigenvalues  $f_{\gamma}$  are computed by diagonalizing the  $\rho$  matrix, and similarly for their perturbation expansion, expressed in terms of Sternheimer equations of different orders. The first-order eigenvalues are found easily using the Hellmann-Feynman theorem [42,43]:

$$f_{\gamma}^{(1)} = \rho_{\gamma\gamma}^{(1)}, \quad (44)$$

while the second-order eigenvalues are obtained as

$$f_{\gamma}^{(2)} = \rho_{\gamma\gamma}^{(2)} - \sum_i^{\text{pocc}'} \frac{|\rho_{i\gamma}^{(1)}|^2}{f_i^{(0)} - f_{\gamma}^{(0)}}, \quad (45)$$

where the prime superscript to the summation sign means that the sum over  $i$  excludes the vanishing denominator case. The latter equation is valid in the nondegenerate case but might be generalized to the degenerate case through degenerate perturbation theory. Equation (45) contains the second-order  $\rho_{\gamma\gamma}^{(2)}$  that must be discarded in the context of the computation of Eq. (42) and its contribution to Eq. (34), as mentioned previously. Thus, the second-order entropy contribution is

$$-TS^{(2)}[\{\rho_{ij}^{(1)}\}] = -kT n_s \left\{ - \sum_{ij}^{\text{pocc}'} s'[f_j^{(0)}] \frac{|\rho_{ij}^{(1)}|^2}{f_i^{(0)} - f_j^{(0)}} + \sum_i^{\text{pocc}} s''[f_i^{(0)}] \frac{[\rho_{ii}^{(1)}]^2}{2} \right\}, \quad (46)$$

where the prime superscript to the summation sign means that the double sum over  $i$  and  $j$  excludes the vanishing denominator case. It can be further worked out, using Eqs. (10) and (32), eliminating the  $s$  function and its derivatives, then using the hermiticity of the  $\hat{\rho}^{(1)}$  operator:

$$-TS^{(2)}[\{\rho_{ij}^{(1)}\}] = -n_s \left\{ \sum_{ij}^{\text{pocc}'} \frac{\epsilon_i^{(0)} - \epsilon_j^{(0)}}{f_i^{(0)} - f_j^{(0)}} \frac{|\rho_{ij}^{(1)}|^2}{2} + \sum_i^{\text{pocc}} \left[ \frac{\partial f}{\partial x} \Big|_{x=\epsilon_i^{(0)} - \mu^{(0)}} \right]^{-1} \frac{[\rho_{ii}^{(1)}]^2}{2} \right\}. \quad (47)$$

With this explicitation of the second-order entropy, the expression of the second-order variational free energy in Eqs. (34)–(36) is complete.

Quadratic terms in  $\{\psi_i^{(1)}\}$  appear in Eq. (35) and in the Hxc contribution, the third term of Eq. (34). Quadratic terms in  $\{\rho_{ij}^{(1)}\}$  appear in the entropy contribution, Eq. (47), as well as in the Hxc contribution. Also, bilinear terms in  $\{\psi_i^{(1)}\}$  and  $\{\rho_{ij}^{(1)}\}$  appear in the second term of Eq. (34) and in the Hxc contribution.

The whole expression must be definitely positive with respect to changes of  $\{\psi_i^{(1)}\}$  and  $\{\rho_{ij}^{(1)}\}$  taken in their quadratic/bilinear contribution. For a monotonically decreasing  $f(x)$  function, the prefactor of  $\rho_{ij}^{(1)}$  or  $\rho_{ii}^{(1)}$  in Eq. (46) [or Eq. (47)] is positive, and these contributions are convex. The situation is also clear for the  $K_H$  contribution to Eq. (34) but not so for the whole  $K_{\text{Hxc}}$ . Indeed, while  $K_H$  is a positive-definite kernel, the kernel  $K_{\text{xc}}$  is not (even  $K_{\text{xc}}$  is definite-negative in the local density approximation). To finalize the analysis of the extremal character of Eq. (34), we also need to address the quadratic term in  $\psi_i^{(1)}$ . This will be done when discussing the gauge choices.

### B. Minimization of the second-order free energy

The second-order free energy  $F^{+(2)}$ , Eq. (34), can now be minimized, by computing the gradients with respect to the variables  $\{\psi_i^{(1)}\}$  and  $\{\rho_{ij}^{(1)}\}$ . The need to impose the Hermitian character of  $\{\rho_{ij}^{(1)}\}$  might seem to yield some complication. However, this can be bypassed by generalizing Eq. (34) to non-Hermitian  $\{\rho_{ij}^{(1)}\}$ , as is done in Supplemental Material [39] Sec. S3. The gradients are explicitly written in Supplemental Material [39] Sec. S4. At the minimum, the gradients vanish, and one finds the following equations, which are independent of the choice of gauge. Depending on the gauge, such expressions might further simplify. This will be seen in Sec. IV.

Imposing zero diagonal occupation gradient delivers

$$\rho_{ii}^{(1)} = \left. \frac{\partial f}{\partial \epsilon} \right|_{\epsilon_i^{(0)} - \mu^{(0)}} [\epsilon_i^{(1)} - \mu^{(1)}], \quad (48)$$

while for the case of off-diagonal occupation gradients, one gets

$$\begin{aligned} \rho_{ij}^{(1)} = & \frac{f_i^{(0)} - f_j^{(0)}}{\epsilon_i^{(0)} - \epsilon_j^{(0)}} \langle \psi_i^{(0)} | \hat{H}^{(1)} | \psi_j^{(0)} \rangle \\ & - [f_i^{(0)} - f_j^{(0)}] [\langle \psi_i^{(1)} | \psi_j^{(0)} \rangle - \langle \psi_i^{(0)} | \psi_j^{(1)} \rangle], \quad (49) \end{aligned}$$

where

$$\hat{H}^{(1)} = \hat{v}_{\text{ext}}^{(1)} + \int K_{\text{Hxc}}[\rho](\mathbf{r}, \mathbf{r}') \rho^{(1)}(\mathbf{r}') d\mathbf{r}'. \quad (50)$$

Imposing zero projected gradient of  $F^{+(2)}$  with respect to  $\langle \psi_i^{(1)} |$  in the  $S_{\text{pocc}}$  space gives an expression for the first-order

Lagrange multipliers:

$$\begin{aligned} \Lambda_{ki}^{(1)} = & f_i^{(0)} \{ [\epsilon_k^{(0)} - \epsilon_i^{(0)}] \langle \psi_k^{(0)} | \psi_i^{(1)} \rangle \\ & + \langle \psi_k^{(0)} | \hat{H}^{(1)} | \psi_i^{(0)} \rangle \} + \rho_{ki}^{(1)} \epsilon_k^{(0)}. \quad (51) \end{aligned}$$

The diagonal elements are

$$\Lambda_{ii}^{(1)} = f_i^{(0)} \epsilon_{ii}^{(1)} + \rho_{ii}^{(1)} \epsilon_i^{(0)}. \quad (52)$$

Imposing zero projected gradient of  $F^{+(2)}$  with respect to  $\langle \psi_i^{(1)} |$  out of the  $S_{\text{pocc}}$  space gives the usual Sternheimer equation of DFPT [4]:

$$\hat{P}_\perp [\hat{H}^{(0)} - \epsilon_i^{(0)}] \hat{P}_\perp | \psi_i^{(1)} \rangle = -\hat{P}_\perp \hat{H}^{(1)} | \psi_i^{(0)} \rangle. \quad (53)$$

This is also directly connected to a key equation in the work of de Gironcoli [3], the projection of his Eq. (11) in the space perpendicular to the active space of unperturbed wave functions.

## IV. THE DIFFERENT GAUGES

### A. The gauge freedom

From the very start, the diagonal gauge has been chosen for the unperturbed wave functions and occupations, namely, Eq. (15), giving Eq. (19) and

$$\rho_{ij}^{(0)} = \delta_{ij} f_i^{(0)}, \quad (54)$$

$$\hat{H}^{(0)} | \psi_j^{(0)} \rangle = \epsilon_j^{(0)} | \psi_j^{(0)} \rangle, \quad (55)$$

and

$$\Lambda_{kj}^{(0)} = f_j^{(0)} \delta_{kj} \epsilon_j^{(0)}. \quad (56)$$

However, no gauge choice has been made for the first-order quantities, while there is indeed a gauge freedom originating from the possibilities of a unitary transform in the starting problem. The constraints (to be fulfilled whatever the gauge) are Eqs. (40) and (41). Equation (40) fixes the symmetric part of the scalar product between the zeroth- and first-order wave functions. However, the asymmetric part of the scalar product between the zeroth- and first-order wave functions is not fixed:

$$\langle \psi_i^{(1)} | \psi_j^{(0)} \rangle - \langle \psi_i^{(0)} | \psi_j^{(1)} \rangle = A_{ij}. \quad (57)$$

We first examine the consequences of choosing  $A_{ij} = 0$ , which is called the parallel gauge for the first-order wave functions, then examine other possibilities. Note that  $\hat{H}^{(1)}$ ,  $\rho^{(1)}$ , and  $F^{(2)}$  must be invariant under such a choice. Section S5 in the Supplemental Material [39] shows how the first-order wave functions and occupation matrix elements change concurrently.

### B. The parallel gauge

First-order wave functions in the parallel gauge are noted  $|\psi_{||,i}^{(1)}\rangle$ , like for the first-order density matrix elements. One imposes

$$\langle \psi_i^{(0)} | \psi_{||,j}^{(1)} \rangle = 0 \quad (58)$$

when  $i$  and  $j \in S_{\text{pocc}}$ . The second-order free energy  $F^{+(2)}$ , Eqs. (34)–(36), simplifies: The last two contributions to Eq. (36) vanish as well as the fifth term of Eq. (34).

One gets

$$F^{+(2)}[T; \{\psi_{\parallel,i}^{(1)}\}; \{\rho_{\parallel,ij}^{(1)}\}] = n_s \sum_i^{\text{pocc}} f_i^{(0)} \{ \langle \psi_{\parallel,i}^{(1)} | \hat{H}^{(0)} - \epsilon_i^{(0)} | \psi_{\parallel,i}^{(1)} \rangle + \langle \psi_i^{(0)} | v_{\text{ext}}^{(2)} | \psi_i^{(0)} \rangle + [ \langle \psi_{\parallel,i}^{(1)} | v_{\text{ext}}^{(1)} | \psi_i^{(0)} \rangle + (\text{c.c.}) ] \} \quad (59a)$$

$$+ n_s \sum_{ij}^{\text{pocc}} \rho_{\parallel,ji}^{(1)} \langle \psi_i^{(0)} | v_{\text{ext}}^{(1)} | \psi_j^{(0)} \rangle + \frac{1}{2} \iint K_{\text{Hxc}}(\mathbf{r}, \mathbf{r}') \rho^{(1)}(\mathbf{r}) \rho^{(1)}(\mathbf{r}') d\mathbf{r} d\mathbf{r}' \quad (59b)$$

$$- \frac{n_s}{2} \sum_{ij}^{\text{pocc}'} \frac{\epsilon_i^{(0)} - \epsilon_j^{(0)}}{f_i^{(0)} - f_j^{(0)}} |\rho_{\parallel,ij}^{(1)}|^2 - \frac{n_s}{2} \sum_i^{\text{pocc}} \frac{\partial \epsilon}{\partial f} \Big|_{f_i^{(0)}} [\rho_{\parallel,ii}^{(1)}]^2 - n_s \mu^{(1)} \sum_i^{\text{pocc}} \rho_{\parallel,ii}^{(1)}. \quad (59c)$$

The analysis of the extremal character of  $F^{+(2)}$ , started at the end of Sec. III A, can be pursued. Indeed, the quadratic term in  $\psi_{\parallel,i}^{(1)}$  in Eq. (59a):

$$\langle \psi_{\parallel,i}^{(1)} | \hat{H}^{(0)} - \epsilon_i^{(0)} | \psi_{\parallel,i}^{(1)} \rangle, \quad (60)$$

is obviously convex since  $\psi_{\parallel,i}^{(1)}$  can be decomposed in the basis of eigenvectors of  $\hat{H}^{(0)}$  and has only components with eigenenergies  $\epsilon_j^{(0)}$  higher (or equal) to  $\epsilon_i^{(0)}$  (see details in Sec. S7 in the Supplemental Material [39]).

The combination of  $K_{\text{Hxc}}$  with the positive-definiteness of Eq. (60) and the ones of Eqs. (59b) and (59c) (discussed at the end of Sec. III A) allows one to better understand the  $F^{(2)}$  extremal character. In any case, this property is also linked to the extremal character of the unperturbed  $F$ .

Let us now examine the equations at the minimum in the parallel gauge. Some of them do not change: Eq. (48) is unchanged, and  $\rho^{(1)}$  is still obtained from Eq. (38). The off-diagonal first-order density matrix gradients, see Eq. (49), are simplified and deliver at the minimum:

$$\rho_{\parallel,ij}^{(1)} = \frac{f_i^{(0)} - f_j^{(0)}}{\epsilon_i^{(0)} - \epsilon_j^{(0)}} \langle \psi_i^{(0)} | \hat{H}^{(1)} | \psi_j^{(0)} \rangle. \quad (61)$$

The projected gradient of the first-order wave functions in the  $S_{\text{pocc}}$  space, Eq. (51), becomes

$$\Lambda_{ki}^{(1)} = f_i^{(0)} \langle \psi_k^{(0)} | \hat{H}^{(1)} | \psi_i^{(0)} \rangle + \rho_{\parallel,ki}^{(1)} \epsilon_k^{(0)}. \quad (62)$$

### C. The diagonal gauge

Is it possible to choose a gauge where all the matrix elements  $\rho_{ij}^{(1)}$  vanish? Indeed, this would bring back the formalism for metals to the one found for gapped systems, without modification of the occupations.

Unfortunately, it is not possible to adjust the diagonal values of  $\rho^{(1)}$  thanks to a choice of gauge. Indeed, whatever the gauge,

$$\rho_{ii}^{(1)} = \rho_{\parallel,ii}^{(1)} = \frac{\partial f}{\partial \epsilon} \Big|_{\epsilon_i^{(0)} - \mu^{(0)}} [\epsilon_i^{(1)} - \mu^{(1)}]. \quad (63)$$

If some states are partially occupied,  $\frac{\partial f}{\partial \epsilon}$  does not vanish, and thus, also  $\rho_{ii}^{(1)}$  does not vanish (except possibly due to symmetry reasons). By contrast, for the nondiagonal elements, it is possible to impose

$$0 = \rho_{\parallel,ji}^{(1)} - \frac{1}{2} A_{ji} [f_j^{(0)} - f_i^{(0)}]. \quad (64)$$

This choice will be called the diagonal gauge. The relation between the diagonal and parallel gauge wave functions is

$$|\psi_{\text{di}}^{(1)}\rangle = |\psi_{\parallel,i}^{(1)}\rangle - \sum_j^{\text{pocc}'} \frac{\langle \psi_j^{(0)} | \hat{H}^{(1)} | \psi_i^{(0)} \rangle}{\epsilon_j^{(0)} - \epsilon_i^{(0)}} |\psi_j^{(0)}\rangle. \quad (65)$$

Then  $|\psi_{\text{di}}^{(1)}\rangle$  fulfills

$$\hat{P}_{\perp,i} [\hat{H}^{(0)} - \epsilon_i^{(0)}] \hat{P}_{\perp,i} |\psi_{\text{di}}^{(1)}\rangle = -\hat{P}_{\perp,i} \hat{H}^{(1)} |\psi_i^{(0)}\rangle, \quad (66)$$

that is, the Sternheimer equation, in the diagonal gauge. The notation  $\hat{P}_{\perp,i}$  is for the projector on the space perpendicular to the unperturbed state  $i$ . Also,

$$\langle \psi_{\text{di}}^{(1)} | \psi_j^{(0)} \rangle + \langle \psi_i^{(0)} | \psi_{\text{di}}^{(1)} \rangle = 0. \quad (67)$$

The second-order free energy can be computed in the diagonal gauge and simplifies due to the constraint in Eq. (67). Equations (34)–(36) become

$$F^{+(2)}[T; \{\psi_{\text{di}}^{(1)}\}, \{\rho_{\text{dii}}^{(1)}\}] = n_s \sum_i^{\text{pocc}} f_i^{(0)} \{ \langle \psi_{\text{di}}^{(1)} | \hat{H}^{(0)} - \epsilon_i^{(0)} | \psi_{\text{di}}^{(1)} \rangle + \langle \psi_i^{(0)} | \hat{v}_{\text{ext}}^{(2)} | \psi_i^{(0)} \rangle + [ \langle \psi_{\text{di}}^{(1)} | \hat{v}_{\text{ext}}^{(1)} | \psi_i^{(0)} \rangle + (\text{c.c.}) ] \} \\ + n_s \sum_i^{\text{pocc}} \rho_{\text{dii}}^{(1)} \langle \psi_i^{(0)} | \hat{v}_{\text{ext}}^{(1)} | \psi_i^{(0)} \rangle + \frac{1}{2} \iint K_{\text{Hxc}}(\mathbf{r}, \mathbf{r}') \rho^{(1)}(\mathbf{r}) \rho^{(1)}(\mathbf{r}') d\mathbf{r} d\mathbf{r}' \\ - \frac{n_s}{2} \sum_i^{\text{pocc}} \frac{\partial \epsilon}{\partial f} \Big|_{f_i^{(0)}} [\rho_{\text{dii}}^{(1)}]^2 - n_s \mu^{(1)} \sum_i^{\text{pocc}} \rho_{\text{dii}}^{(1)}, \quad (68)$$

with

$$\rho^{(1)}(\mathbf{r}) = n_s \left\{ \sum_i^{\text{pocc}} \rho_{\text{dii}}^{(1)} \psi_i^{*(0)}(\mathbf{r}) \psi_i^{(0)}(\mathbf{r}) + f_i^{(0)} [\psi_{\text{di}}^{*(1)}(\mathbf{r}) \psi_i^{(0)}(\mathbf{r}) + \psi_i^{*(0)}(\mathbf{r}) \psi_{\text{di}}^{(1)}(\mathbf{r})] \right\}. \quad (69)$$

Note the presence of only the diagonal elements of  $\rho^{(1)}$  in both Eqs. (68) and (69).

#### D. Complete suppression of first-order occupation matrix elements

The diagonal gauge is numerically inconvenient because of the presence of the denominator  $\epsilon_j^{(0)} - \epsilon_i^{(0)}$  in Eq. (65), so that the corresponding term can become very large for small differences, while the contributions of pairs  $ij$  and  $ji$  will nearly cancel each other in Eqs. (67) and (69). Also, one would prefer to use the same formula (hence the same coding) to build  $\rho^{(1)}(\mathbf{r})$  as in the case of insulators, with the only modification being the presence of occupation numbers:

$$\rho^{(1)}(\mathbf{r}) = n_s \sum_i^{\text{pocc}} f_i^{(0)} [\psi_{\text{mod},i}^{*(1)}(\mathbf{r}) \psi_i^{(0)}(\mathbf{r}) + \psi_i^{*(0)}(\mathbf{r}) \psi_{\text{mod},i}^{(1)}(\mathbf{r})]. \quad (70)$$

This can be achieved as follows. Instead of Eq. (65), one defines

$$\begin{aligned} |\psi_{\text{mod},i}^{(1)}\rangle &= |\psi_{\parallel,i}^{(1)}\rangle + \sum_j^{\text{pocc}} \Theta[f_i^{(0)}, f_j^{(0)}] \\ &\quad \times \frac{f_j^{(0)} - f_i^{(0)}}{f_i^{(0)}} \frac{\langle \psi_j^{(0)} | \hat{H}^{(1)} | \psi_i^{(0)} \rangle}{\epsilon_j^{(0)} - \epsilon_i^{(0)}} |\psi_j^{(0)}\rangle, \end{aligned} \quad (71)$$

where  $\Theta[f_i^{(0)}, f_j^{(0)}]$ , to be defined later, is such that

$$\Theta[f_i^{(0)}, f_j^{(0)}] + \Theta[f_j^{(0)}, f_i^{(0)}] = 1, \quad (72)$$

$$\Theta[f_i^{(0)} = 0, f_j^{(0)}] = 0. \quad (73)$$

This allows one to avoid the divergence in Eq. (71). Note that, when  $f_i^{(0)} = f_j^{(0)}$ ,

$$\Theta[f_i^{(0)}, f_j^{(0)}] = \frac{1}{2}. \quad (74)$$

Also, in Eq. (71), one has to understand that

$$\frac{f_j^{(0)} - f_i^{(0)}}{\epsilon_j^{(0)} - \epsilon_i^{(0)}} = \left. \frac{\partial f}{\partial \epsilon} \right|_{\epsilon_i^{(0)}} \quad (75)$$

when  $\epsilon_j^{(0)} = \epsilon_i^{(0)}$ .

In principle, the occupation numbers are positive, but this is broken in case of advanced smearing schemes. Thus, the function  $\Theta$  should also be defined outside of the  $0 \leq f^{(0)} \leq 1$  range.

In the Supplemental Material [39], Sec. S6, it is checked that the condition expressed by Eq. (72) insures that the computation of Eq. (70) delivers the correct  $\rho^{(1)}$ , equal to the one obtained in the parallel gauge. Similarly, one can show that the terms linear in  $\psi_i^{(1)}$  and  $\rho_{ji}^{(1)}$  in Eq. (59a) are equivalent in the parallel gauge or with the modified wave functions. By contrast, for the evaluation of  $F^{+(2)}$ , the quadratic terms in  $\psi_{\parallel,i}^{(1)}$  in Eq. (59a) are not left invariant. Instead of correcting them, it is better to stick with the formula for  $F^{+(2)}$  in the parallel gauge.

In ABINIT, the following  $\Theta$  function is implemented:

$$\Theta(f_i, f_j) = H(|f_i| - |f_j|), \quad (76)$$

where  $H(x)$  is the Heaviside step function, with value  $\frac{1}{2}$  at  $x = 0$ :

$$H(x) = \begin{cases} 1 & x > 0 \\ \frac{1}{2} & x = 0 \\ 0 & x < 0. \end{cases} \quad (77)$$

The advantage of this formulation, beyond satisfying Eqs. (72) and (73) trivially, comes from the fact that the sum  $\sum_j^{\text{pocc}}$  in Eq. (71) includes only the wave functions  $|\psi_j^{(0)}\rangle$  with absolute occupation lower than the one of  $|\psi_i^{(0)}\rangle$ , which translates usually [when  $f(\epsilon)$  is a monotonically decreasing function of  $\epsilon$ , bounded by 0 and 1] into energy  $\epsilon_j^{(0)}$  higher than  $\epsilon_i^{(0)}$ . This yields some CPU time savings, about a factor of two in that operation, instead of doing the sum  $\sum_j^{\text{pocc}}$  on all states.

In practice, the parallel gauge first-order wave functions  $|\psi_{\parallel,i}^{(1)}\rangle$  are computed, at fixed  $\hat{H}^{(1)}$ , and then  $|\psi_{\text{mod},i}^{(1)}\rangle$  is computed, which allows us afterwards to compute  $\rho^{(1)}$ . The computation of the second-order free energy can be done using the parallel gauge formula Eqs. (59a)–(59c), which is variational.

## V. PERIODIC SYSTEMS

Although the occupation numbers and the density matrix have been explicitly treated, the DFT and DFPT formulas presented until now are valid for the case of finite systems, with a set of discretized levels where the occupation number varies with temperature according to the FD statistics. Systems are now treated with lattice periodicity, hence corresponding to the case of extended metals. The above theory is adapted to such a case, with treatment of Brillouin zone integral and the appearance of a continuous band structure as a function of the wave vector. Notations are obvious adaptations to the metallic case of those from Ref. [5], Appendix A. One focuses first on DFT then on DFPT.

### A. DFT for metallic periodic systems

The DFT electronic free energy per unit cell is written

$$F[T; \{u_{n\mathbf{k}}\}, \{\rho_{nm\mathbf{k}}\}] = \frac{n_s \Omega_0}{(2\pi)^3} \int_{\text{BZ}} \sum_{nm} \rho_{nm\mathbf{k}} \langle u_{m\mathbf{k}} | \hat{K}_{\mathbf{k}\mathbf{k}} + \hat{v}_{\text{ext},\mathbf{k}\mathbf{k}} | u_{n\mathbf{k}} \rangle d\mathbf{k} + E_{\text{Hxc}}[\rho] - TS[\{\rho_{nm\mathbf{k}}\}]. \quad (78)$$

This is a generalization of Eq. (1) to periodic solids. The matrix element of the kinetic operator and external potential operator is evaluated over the primitive cell with volume  $\Omega_0$ . The Hartree and exchange-correlation energy  $E_{\text{Hxc}}[\rho]$  is also evaluated for one primitive cell as well as for the entropy. The  $u$ 's are periodic parts of Bloch wave functions. The wave vector  $\mathbf{k}$  integral is performed over the Brillouin zone, with volume  $\frac{(2\pi)^3}{\Omega_0}$ . Here,  $n$  and  $m$  are band indices. The expression of the electronic density is

$$\rho(\mathbf{r}) = \frac{n_s}{(2\pi)^3} \int_{\text{BZ}} \sum_{nm} \rho_{nm\mathbf{k}} u_{m\mathbf{k}}^*(\mathbf{r}) u_{n\mathbf{k}}(\mathbf{r}) d\mathbf{k}. \quad (79)$$

In Eqs. (78) and (79), the wave functions are normalized as follows:

$$\langle u_{m\mathbf{k}} | u_{n\mathbf{k}} \rangle = \frac{1}{\Omega_0} \int_{\Omega_0} u_{m\mathbf{k}}(\mathbf{r})^* u_{n\mathbf{k}}(\mathbf{r}) d\mathbf{r} = \delta_{mn}. \quad (80)$$

The Hamiltonian and occupation matrix can be simultaneously diagonalized, as in the discrete situation, with

$$\begin{aligned} \hat{H}_{\mathbf{k}\mathbf{k}} | u_{n\mathbf{k}} \rangle &= (\hat{K}_{\mathbf{k}\mathbf{k}} + \hat{v}_{\text{ext},\mathbf{k}\mathbf{k}} + \hat{v}_{\text{Hxc},\mathbf{k}\mathbf{k}}[\rho]) | u_{n\mathbf{k}} \rangle \\ &= \epsilon_{n\mathbf{k}} | u_{n\mathbf{k}} \rangle. \end{aligned} \quad (81)$$

Minimization of the free energy yields the same relationship between the eigenenergy and occupation number as in the discrete case, Eq. (12).

In this diagonal gauge, the Brillouin zone integral entering the electronic density can be transformed to an energy integral, as follows. The energy-resolved electronic density is defined as

$$\rho(\mathbf{r}, \epsilon) = \frac{n_s}{(2\pi)^3} \int_{\text{BZ}} \sum_n \delta(\epsilon - \epsilon_{n\mathbf{k}}) u_{n\mathbf{k}}^*(\mathbf{r}) u_{n\mathbf{k}}(\mathbf{r}) d\mathbf{k}, \quad (82)$$

such that

$$\rho(\mathbf{r}) = \int_{-\infty}^{+\infty} f\left(\frac{\mu - \epsilon}{kT}\right) \rho(\mathbf{r}, \epsilon) d\epsilon. \quad (83)$$

### B. DFPT for metallic periodic systems

DFPT for periodic systems allows one to treat perturbations that are characterized by a wave vector  $\mathbf{q}$ : Like Bloch wave functions, they have a periodic part and a phase. In Sec. IV of Ref. [5], the strategy to deal with such generic perturbations is explained and involves factorizing the phase in all DFPT equations. We keep the same notations as in that reference and proceed with the systematic generalization of the quantities developed in the DFPT for varying occupations, as obtained in the previous sections, for the parallel gauge case. The generalization to other gauges proceeds in a similar way.

Starting with first-order quantities, one finds that Eq. (58) becomes

$$\langle u_{m\mathbf{k}+\mathbf{q}}^{(0)} | u_{||,n\mathbf{k},\mathbf{q}}^{(1)} \rangle = 0 \quad [m, n \in S_{\text{pocc}}], \quad (84)$$

which is like eq. (43) of Ref. [5]. For Eq. (61), one defines

$$\epsilon_{m\mathbf{k}+\mathbf{q},n\mathbf{k}}^{(1)} = \langle u_{m\mathbf{k}+\mathbf{q}}^{(0)} | \hat{H}_{\mathbf{k}+\mathbf{q},\mathbf{k}}^{(1)} | u_{n\mathbf{k}}^{(0)} \rangle, \quad (85)$$

then

$$\rho_{||,m\mathbf{k}+\mathbf{q},n\mathbf{k}}^{(1)} = \frac{f_{m\mathbf{k}+\mathbf{q}}^{(0)} - f_{n\mathbf{k}}^{(0)}}{\epsilon_{m\mathbf{k}+\mathbf{q}}^{(0)} - \epsilon_{n\mathbf{k}}^{(0)}} \epsilon_{m\mathbf{k}+\mathbf{q},n\mathbf{k}}^{(1)}. \quad (86)$$

Equation (38) becomes (see eq. (44) of Ref. [5]):

$$\bar{\rho}_{\mathbf{q}}^{(1)}(\mathbf{r}) = \frac{1}{(2\pi)^3} \int_{\text{BZ}} n_s \left[ \sum_{nm}^{\text{pocc}} \rho_{||,m\mathbf{k}+\mathbf{q},n\mathbf{k}}^{(1)} u_{n\mathbf{k}}^{*(0)}(\mathbf{r}) u_{m\mathbf{k}+\mathbf{q}}^{(0)}(\mathbf{r}) + 2 \sum_m^{\text{pocc}} f_{m\mathbf{k}}^{(0)} u_{m\mathbf{k}}^{*(0)}(\mathbf{r}) u_{m\mathbf{k},\mathbf{q}}^{(1)}(\mathbf{r}) \right] d\mathbf{k}, \quad (87)$$

where  $\bar{\rho}_{\mathbf{q}}^{(1)}(\mathbf{r})$  is the periodic part of the first-order density change. The Sternheimer equation in the periodic case, coming from Eq. (53), is

$$\hat{P}_{\perp\mathbf{k}+\mathbf{q}} [\hat{H}_{\mathbf{k}+\mathbf{q},\mathbf{k}+\mathbf{q}}^{(0)} - \epsilon_{m\mathbf{k}}^{(0)}] \hat{P}_{\perp\mathbf{k}+\mathbf{q}} | u_{||,m\mathbf{k},\mathbf{q}}^{(1)} \rangle = -\hat{P}_{\perp\mathbf{k}+\mathbf{q}} \hat{H}_{\mathbf{k}+\mathbf{q},\mathbf{k}}^{(1)} | u_{m\mathbf{k}}^{(0)} \rangle, \quad (88)$$

where

$$\hat{H}_{\mathbf{k}+\mathbf{q},\mathbf{k}}^{(1)} = \hat{v}_{\text{ext},\mathbf{k}+\mathbf{q},\mathbf{k}}^{(1)} + \int K_{\text{Hxc}}[\rho](\mathbf{r}, \mathbf{r}') \bar{\rho}_{\mathbf{q}}^{(1)}(\mathbf{r}') \exp[-i\mathbf{q}(\mathbf{r} - \mathbf{r}')] d\mathbf{r}'. \quad (89)$$

Equations (88) and (89), respectively, can be compared with Eqs. (45) and (46) of Ref. [5]. The two Sternheimer equations are identical, while the definition of  $\hat{H}_{\mathbf{k}+\mathbf{q},\mathbf{k}}^{(1)}$  is similar, although in Ref. [5], an additional term is also coming from a possible dependence of the Hartree and exchange-correlation potential on the perturbation, neglected in the present account for the sake of simplicity but implemented in ABINIT.

Let us now examine the second-order free energy  $F^{+(2)}$ . For a nonperiodic perturbation, i.e.,  $\mathbf{q} \neq 0$ , all diagonal elements of  $\epsilon^{(1)}$  or  $\rho_{||}^{(1)}$  vanish. For such a case, Eq. (59c) becomes

$$\begin{aligned}
 & F_{el,-\mathbf{q},\mathbf{q}}^{+(2)}[T, \{u_{||}^{(1)}\}, \{\rho_{||}^{(1)}\}] \\
 &= \frac{\Omega_0}{(2\pi)^3} \int_{\text{BZ}} n_s \left\{ \sum_m^{\text{pocc}} f_{m\mathbf{k}}^{(0)} F_{m\mathbf{k}}^{(2)}[u_{||}^{(1)}] + \frac{1}{2} \sum_{mn}^{\text{pocc}} \left[ \rho_{||,n\mathbf{k},m\mathbf{k}+\mathbf{q}}^{(1)} \langle u_{m,\mathbf{k}+\mathbf{q}}^{(0)} | \hat{v}_{\text{ext},\mathbf{k}+\mathbf{q},\mathbf{k}}^{(1)} | u_{n\mathbf{k}}^{(0)} \rangle + (\text{c.c.}) \right] \right\} d\mathbf{k} \\
 &+ \frac{1}{2} \int_{\Omega_0} \int K_{\text{Hxc}}(\mathbf{r}, \mathbf{r}') \bar{\rho}_{\mathbf{q}}^{*(1)}(\mathbf{r}) \bar{\rho}_{\mathbf{q}}^{(1)}(\mathbf{r}') \exp[-i\mathbf{q}(\mathbf{r} - \mathbf{r}')] d\mathbf{r} d\mathbf{r}' - \frac{n_s}{2} \frac{\Omega_0}{(2\pi)^3} \int_{\text{BZ}} \sum_{mn}^{\text{pocc}} \frac{\epsilon_{m,\mathbf{k}+\mathbf{q}}^{(0)} - \epsilon_{n\mathbf{k}}^{(0)}}{f_{m,\mathbf{k}+\mathbf{q}}^{(0)} - f_{n\mathbf{k}}^{(0)}} |\rho_{||,m\mathbf{k}+\mathbf{q},n\mathbf{k}}^{(1)}|^2 d\mathbf{k}, \quad (90)
 \end{aligned}$$

where

$$\begin{aligned}
 F_{m\mathbf{k}}^{(2)}[u_{||}^{(1)}] &= \langle u_{||,m\mathbf{k},\mathbf{q}}^{(1)} | \hat{H}_{\mathbf{k}+\mathbf{q},\mathbf{k}+\mathbf{q}}^{(0)} - \epsilon_{m\mathbf{k}}^{(0)} | u_{||,m\mathbf{k},\mathbf{q}}^{(1)} \rangle \\
 &+ \langle u_{m\mathbf{k}}^{(0)} | \hat{v}_{\text{ext},\mathbf{k},\mathbf{k}}^{(2)} | u_{m\mathbf{k}}^{(0)} \rangle \\
 &+ [\langle u_{||,m\mathbf{k},\mathbf{q}}^{(1)} | \hat{v}_{\text{ext},\mathbf{k}+\mathbf{q},\mathbf{k}}^{(1)} | u_{m\mathbf{k}}^{(0)} \rangle + (\text{c.c.})]. \quad (91)
 \end{aligned}$$

Equations (90) and (91) can be compared with Eq. (42) in Ref. [5]. In the latter, three additional terms also come from a possible dependence of the Hartree and exchange-correlation potential on the perturbation, also not included in the present account, like in the equation for the first-order Hamiltonian. Also, the dependence of  $F_{el,-\mathbf{q},\mathbf{q}}^{+(2)}$  on  $\mathbf{q}$  is not mentioned in Eq. (90), for the sake of simplicity. By the same token, the  $\mathbf{q}$  dependence is also not indicated for the second-order  $F_{m\mathbf{k}}^{(2)}$ . By contrast,  $\hat{v}_{\text{ext},\mathbf{k},\mathbf{k}}^{(2)}$  has no  $\mathbf{q}$  dependence, see Eq. (49) in Ref. [5].

The commensurate perturbation case, that is, either  $\mathbf{q} = 0$ , or  $\mathbf{q}$  is a vector of the reciprocal lattice, is quite similar to the case of finite systems, so the explicit formula is obvious and will not be written here.

## VI. APPLICATIONS

As mentioned in the introduction, there have been many different applications of the formalism presented in the previous sections. However, in such studies, usually, results have been presented with little or no emphasis on understanding and characterizing the convergence characteristics with respect to the temperature (or with respect to the smearing energy) jointly with the sampling of the Brillouin zone. Interestingly, the target precision of the calculation, or its purpose, is seen to play an important role in the definition of the convergence regime.

In the following, the phonon frequencies of copper at the  $X$  point in the Brillouin zone, for both transverse and longitudinal modes, are taken as examples. The Perdew-Burke-Ernzerhof exchange-correlation functional is used, with the optimized norm-conserving Vanderbilt pseudopotential [44] from the PSEUDO-DOJO [45], and an energy cutoff of 46.0 Ha. Bulk copper metal is face-centered cubic, with optimized lattice parameter 3.63 Å for the conventional cell edge. Calculations have been done with ABINIT v9.8.3.

Computing the phonon frequencies is often done with a target of 1 cm<sup>-1</sup>. This will be our reference target indeed for this property. Such precision is not difficult to reach and corresponds to a range of parameters that might be called

medium precision. However, one might also be interested in the examination of the specific change of phonon frequencies as a function of electronic temperature. The changes are much smaller, and it is much more demanding to reliably obtain such temperature dependence. This regime is called high precision.

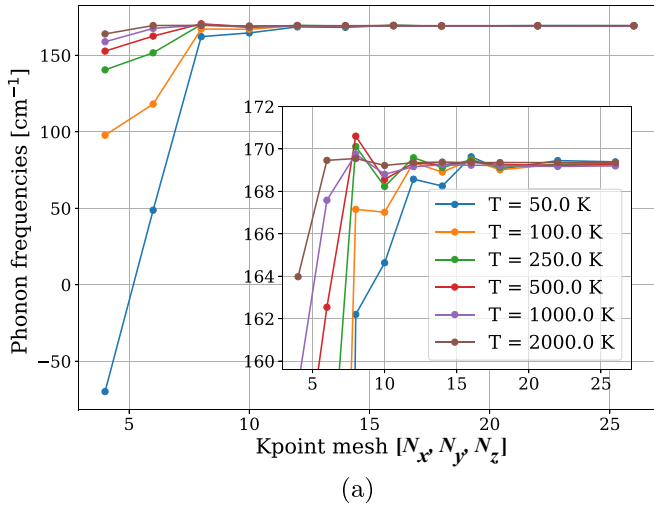
In Fig. 2, the phonon frequencies are presented, as a function of the discreteness of the grid used to sample the Brillouin zone. One targets the estimation of the phonon frequencies at 0 K. The FD broadening is used here only for the purpose of alleviating some of the numerical burden.

The precision obtained for the longitudinal and transverse frequencies, for the same parameters of the computation, is quite different. With the coarse 4 × 4 × 4 mesh at the lowest temperature (50 K), the longitudinal frequency (lower panel) is not so bad and already close to the target precision of 1 cm<sup>-1</sup>. At variance, for such a coarse grid, the transverse frequency is hardly significant. Moreover, the computation of the low-temperature phonon frequencies does not need a low temperature: Indeed, for the larger grid used in Fig. 2, 26 × 26 × 26, it is seen that the effect of the temperature is very small; going from 50 to 2000 K modifies the phonon frequencies by ≪ 1 cm<sup>-1</sup> for such a grid. Hence, the large smearing temperature of 2000 K can be used for the coarser grids; the low-temperature phonon frequency is obtained well within the target precision of 1 cm<sup>-1</sup>.

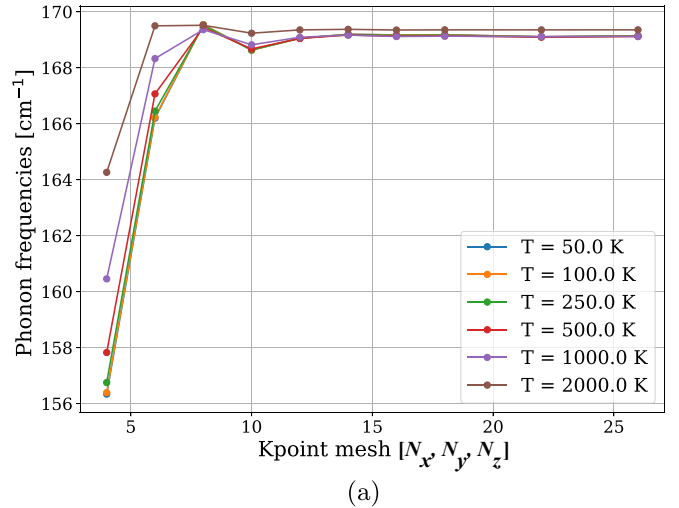
Being more quantitative, with a small broadening temperature of 50 K, one needs a 16 × 16 × 16 wave vector grid to reach the target precision for the transverse mode frequency (see the inset), while for a broadening temperature of 2000 K, the same precision is obtained with a 8 × 8 × 8 wave vector grid. This amounts to a large savings of computational resources. Computing time and memory (or disk space) scale indeed linearly with the number of wave vectors in the Brillouin zone. Hence, the speed-up obtained by using the coarser grid instead of the fine grid is about an order of magnitude.

Figure 3 presents results obtained with the resmearing scheme (FD statistics and MP smearing), where the MP smearing parameters correspond to a temperature of 3000 K. One sees that, irrespective of the physical electronic temperature value, the phonon frequencies are converged within the target value for a 8 × 8 × 8 wave vector grid.

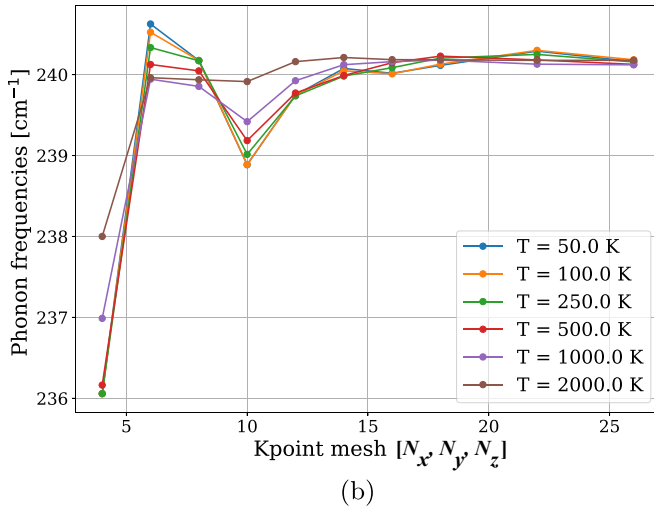
Let us now turn to the high-precision regime, for which the target is to obtain the change of phonon frequencies as a function of the physical electronic temperature. Using the 4 × 4 × 4, 8 × 8 × 8, or 16 × 16 × 16 wave vector grid does



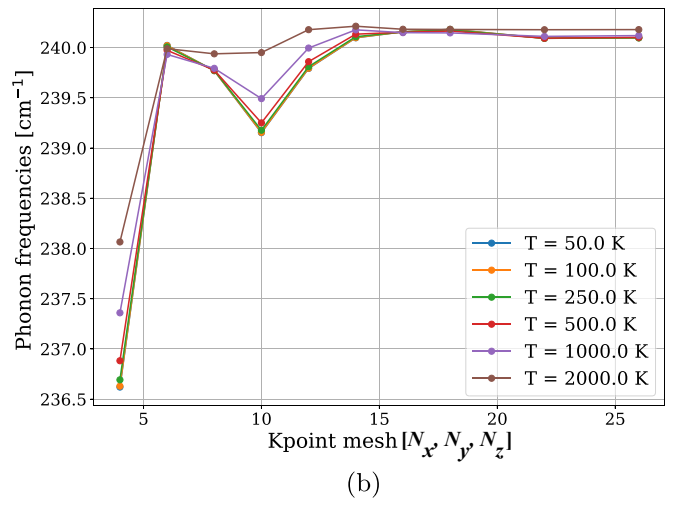
(a)



(a)



(b)



(b)

FIG. 2. Phonon frequencies as a function of the wave vector mesh, using the Fermi-Dirac statistics, across a range of physical electronic temperatures (50–2000 K). The inset provides a closer view of the 160–172  $\text{cm}^{-1}$  range. The horizontal axis defines the linear discretization  $N_x = N_y = N_z$  of these three-dimensional wave vector meshes  $[N_x, N_y, N_z]$ . (a) Transverse phonon frequencies (b) Longitudinal phonon frequencies.

not yield meaningful temperature dependence of these phonon frequencies. Such a temperature dependence can be obtained with much finer grids of  $30 \times 30 \times 30$  or even  $42 \times 42 \times 42$  (for the latter, see Supplemental Material [39] Sec. S8).

Figure 4 presents the phonon frequencies as a function of the physical temperature, for different values of the MP broadening parameter, again for the transverse as well as longitudinal phonon modes. The scale of this figure is quite different than the previous figures. Indeed, the change of phonon frequencies from a low temperature to the highest temperature (2000 K) is on the order of  $0.5 \text{ cm}^{-1}$  for the frequency of the transverse mode and even smaller for the frequency of the longitudinal mode, as seen previously. Thus, the target precision must be much smaller as well. Having in mind the description of the global behavior, one sees that, for MP broadening  $< 3000\text{--}4000$  K, at small physical electronic temperature, there are considerable deviations from the

FIG. 3. Phonon frequencies as a function of the wave vector mesh obtained with the resmearing scheme (broadening value 3000 K), across physical electronic temperatures from 50 to 2000 K. The horizontal axis defines the linear discretization  $N_x = N_y = N_z$  of these three-dimensional wave vector meshes  $[N_x, N_y, N_z]$ . (a) Transverse phonon frequencies (b) Longitudinal phonon frequencies.

expected parabolic behavior, for this very fine  $30 \times 30 \times 30$  wave vector grid. In Sec. S8 in the Supplemental Material [39], an even finer  $42 \times 42 \times 42$  grid is used. However, without MP broadening, the behavior is not guaranteed to be even qualitatively correct. We have not pushed beyond such a  $42 \times 42 \times 42$  grid.

## VII. UNDERCONVERGED GROUND-STATE WAVE FUNCTIONS

Until now, all the formulas in DFPT assume that the unperturbed wave functions  $\psi_i^{(0)}$  are perfect solutions to the unperturbed Schrödinger equation. In practice, while the occupied ones are usually excellent indeed, the unoccupied ones can be loosely converged since they do not contribute to the ground-state unperturbed total energy or density. They might be more difficult to converge than the lower-lying ones, espe-

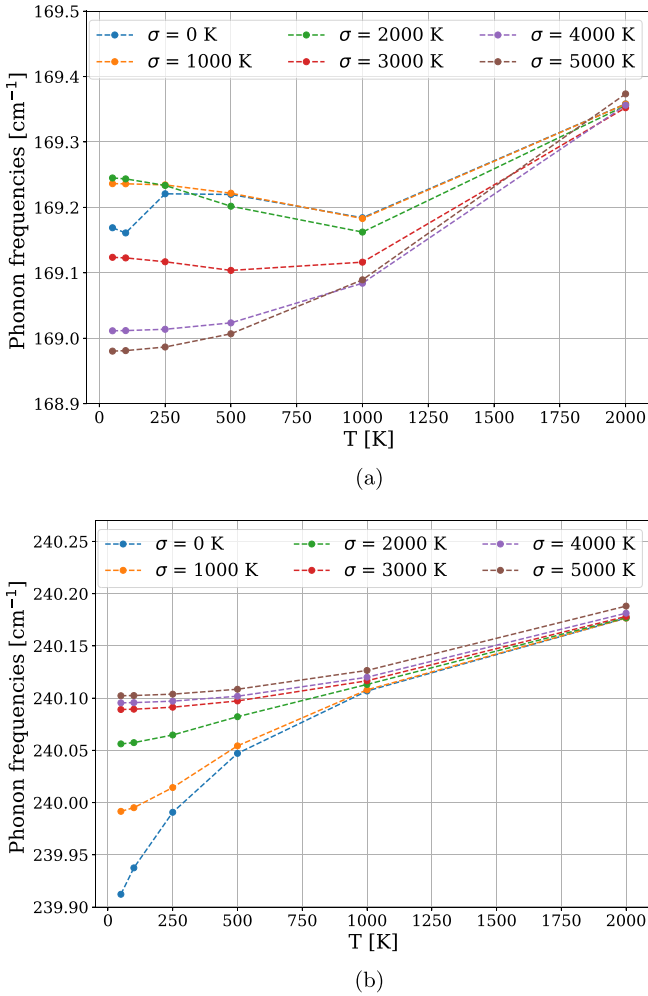


FIG. 4. Phonon frequencies obtained from various Methfessel-Paxton (MP) broadening values (0–5000 K), as a function of physical electronic temperatures (50–2000 K), obtained with a  $30 \times 30 \times 30$  wave vector grid. (a) Transverse phonon frequencies (b) Longitudinal phonon frequencies.

cially if there is a degeneracy between the highest state in the partially occupied space and the lowest state outside of it.

However, in DFPT, slightly incorrect  $\psi_i^{(0)}$  in the partly occupied space [or even  $\psi_i^{(0)}$  associated with vanishing occupations] will induce proportional errors in  $F^{(2)}$ . This can be seen and quantified, as shown hereafter, analytically in a simple model as well as numerically.

Let us first examine a three-state model in the noninteracting case. The three exact eigenstates are denoted  $|\psi_1^{(0)}\rangle$ ,  $|\psi_2^{(0)}\rangle$ , and  $|\psi_3^{(0)}\rangle$  with exact eigenvalues  $\epsilon_1^{(0)}$ ,  $\epsilon_2^{(0)}$ , and  $\epsilon_3^{(0)}$ .

The first state occupation number is  $1 - \delta f$ , where  $\delta f$  is not very large but still finite, while the second state occupation number is  $\delta f$ , and the third state is unoccupied. This is the  $S_{\text{pocc}}$  space of the problem.

The ground-state total energy of this independent-particle system, considering the spin degeneracy, as done in the previous sections, is

$$E^{(0)} = n_s [(1 - \delta f)\epsilon_1^{(0)} + \delta f\epsilon_2^{(0)}]. \quad (92)$$

The perturbation couples the different states, with matrix elements denoted

$$H_{ij} = \langle \psi_i^{(0)} | \hat{H}^{(1)} | \psi_j^{(0)} \rangle. \quad (93)$$

The computation of  $E^{(2)}$  gives

$$\begin{aligned} E^{(2)} &= \frac{n_s}{2} \sum_{i \neq j} \frac{f_i^{(0)} - f_j^{(0)}}{\epsilon_i^{(0)} - \epsilon_j^{(0)}} |\langle \psi_i^{(0)} | \hat{H}^{(1)} | \psi_j^{(0)} \rangle|^2 \\ &= n_s \left[ \frac{2\delta f - 1}{\epsilon_2^{(0)} - \epsilon_1^{(0)}} |H_{12}|^2 - \frac{1 - \delta f}{\epsilon_3^{(0)} - \epsilon_1^{(0)}} |H_{13}|^2 \right. \\ &\quad \left. - \frac{\delta f}{\epsilon_3^{(0)} - \epsilon_2^{(0)}} |H_{23}|^2 \right], \quad (94) \end{aligned}$$

with the hypothesis that the occupation numbers are frozen (this hypothesis might be removed and does not affect the final proportionality relation).

Now let us suppose that the ground-state Schrödinger equation has not been solved exactly but approximately, so that there is a small contamination of the second eigenvector  $|\psi_2^{(0)}\rangle$  by the third eigenvector  $|\psi_3^{(0)}\rangle$  and vice versa. The contaminated quantities are denoted with a tilde. This contamination is determined by the admixture angle  $\alpha$ , which should be small:

$$|\tilde{\psi}_2^{(0)}\rangle = \cos \alpha |\psi_2^{(0)}\rangle + \sin \alpha |\psi_3^{(0)}\rangle. \quad (95)$$

Similarly, the third eigenvector is contaminated by  $|\psi_2^{(0)}\rangle$ , and both contaminated vectors are kept orthogonal:

$$|\tilde{\psi}_3^{(0)}\rangle = -\sin \alpha |\psi_2^{(0)}\rangle + \cos \alpha |\psi_3^{(0)}\rangle. \quad (96)$$

The error in the second eigenvector is quantified in terms of its residual  $|R_2\rangle$  defined as

$$|R_2\rangle = [\hat{H}^{(0)} - \tilde{\epsilon}_2^{(0)}] |\tilde{\psi}_2^{(0)}\rangle, \quad (97)$$

where

$$\tilde{\epsilon}_2^{(0)} = \langle \tilde{\psi}_2^{(0)} | \hat{H}^{(0)} | \tilde{\psi}_2^{(0)} \rangle. \quad (98)$$

The norm of the residual vector (or its square) of an approximate eigenvector is a common measure of the convergence of a solution of the Schrödinger equation.

After some intermediate calculation (see Sec. S9 in the Supplemental Material [39]), the squared norm  $R^2$  of the residual of the second eigenvector is obtained:

$$R_2^2 = \langle R_2 | R_2 \rangle = \cos^2 \alpha \sin^2 \alpha [\epsilon_3^{(0)} - \epsilon_2^{(0)}]^2. \quad (99)$$

It is proportional to  $\sin^2 \alpha$ , hence the square of the admixture angle when the latter is small.

Then the contaminated, approximate, second-order derivative of the energy is computed, starting from

$$\tilde{E}^{(2)} = \frac{n_s}{2} \sum_{i \neq j} \frac{f_i^{(0)} - f_j^{(0)}}{\tilde{\epsilon}_i^{(0)} - \tilde{\epsilon}_j^{(0)}} |\langle \tilde{\psi}_i^{(0)} | \hat{H}^{(1)} | \tilde{\psi}_j^{(0)} \rangle|^2. \quad (100)$$

For the three-state model,  $\tilde{\epsilon}_1^{(0)} = \epsilon_1^{(0)}$  (no contamination),  $\tilde{\epsilon}_2^{(0)}$  is given by Eq. (98), and a similar formula holds for  $\tilde{\epsilon}_3^{(0)}$ . This expression is worked out, see Sec. S9 in the Supplemental Material [39], and a Taylor expansion of  $\tilde{E}^{(2)}$  in terms of the small admixture angle is performed, where quadratic contributions are discarded (e.g.,  $\cos^2 \alpha \simeq 1$ ).

After such computation, the difference between the approximate  $\tilde{E}^{(2)}$  and  $E^{(2)}$  is found:

$$\begin{aligned} \tilde{E}^{(2)} - E^{(2)} &\cong n_s 2 \sin \alpha \Re(H_{12}^* H_{13}) \\ &\times \left[ \frac{-1 + 2\delta f}{\epsilon_2^{(0)} - \epsilon_1^{(0)}} + \frac{1 - \delta f}{\epsilon_3^{(0)} - \epsilon_1^{(0)}} \right] + O(\sin^2 \alpha). \end{aligned} \quad (101)$$

Thus, the error  $\tilde{E}^{(2)} - E^{(2)}$  is proportional to the admixture angle, not to its square. This is at variance with the error of  $E^{(2)}$  with respect to an error in  $\psi^{(1)}$  since  $E^{(2)}$  is variational with respect to  $\psi^{(1)}$ . It emphasizes that the determination of eigenvectors in the potentially occupied space must be rather accurate for  $E^{(2)}$  to be accurate. Ignoring prefactors, improving  $R^2$  by  $\sim 10^{-6}$  brings only  $10^{-3}$  decrease of the difference  $\tilde{E}^{(2)} - E^{(2)}$ .

Also, Eq. (101) reveals that, in this three-band model, an error is present even if  $\delta f = 0$ , provided  $\epsilon_2^{(0)} \neq \epsilon_3^{(0)}$ . For the more general many-band case, there will always be unoccupied states with different energies, so that the outcome of this analysis is that, whatever occupation, metallic or insulating materials, if some states in the space of explicitly treated unperturbed wave functions are approximate, there will be nonnegligible errors. Finally, the  $\Re(H_{12}^* H_{13})$  factors indicate that an interference effect between the transition from state 1 to state 2 and the transition from state 1 to state 3 is at the origin of the dominant error.

To substantiate these statements, numerical tests have been made, in which the convergence of the explicitly treated highest-lying states was not perfect, and the second-order derivative of the total energy error was monitored.

As for the previous section, calculations were done for phonon frequencies in copper. The plane-wave kinetic energy cutoff was 50 Ha, and a  $12 \times 12 \times 12$  wave vector grid was used for the Brillouin zone sampling. Phonon calculations were done on a  $6 \times 6 \times 6$  phonon wave vector sampling grid to accumulate statistics. In the ground-state calculations, the number of explicitly treated bands was varied between 10 and 22. A stringent convergence criterion was set for the potential residual at  $10^{-20}$ , ensuring precise results for the potential and density. Still, the higher-lying bands that do not contribute to the density were not fully converged. We systematically varied the number of line steps for the conjugate gradient minimization in the Sternheimer equation from 4 to 18 and monitored the maximum of the square of the wave function residuals. Figure 5 collects the resulting errors in the second-order derivative of the free energy for a whole set of elements of the dynamical matrices as a function of the maximum squared wave function residual. The global trend is in line with the expectations, namely, the maximum absolute error is roughly proportional to square root of the the maximum squared wave function residual (or equivalently proportional to the wave function residual). When the maximum squared residual is  $< \sim 10^{-13}$ , the maximum absolute error saturates at  $\sim 10^{-8}$  Ha. Without having pursued this matter further, it seems plausible that sources of errors independent of the wave function residual exist at that numerical level and start to dominate.

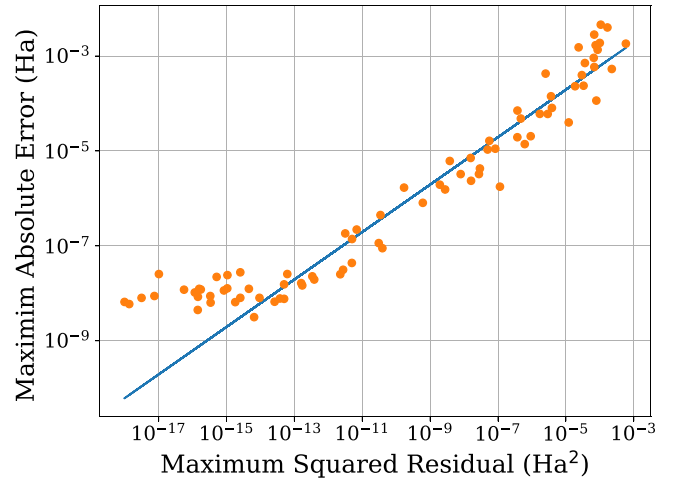


FIG. 5. Relationship between the resulting errors in the second-order derivative of the free energy and the square of the wave function residual. The scatter plot illustrates the observed errors, while the solid line corresponds to a square root behavior.

## VIII. CONCLUSIONS

In this paper, a variational formulation of DFPT for metals has been described, covering in detail the consequences of the presence of an entropy contribution; different smearing schemes, including a resmearing scheme to deal with finite temperatures; the treatment of the space of potentially occupied wave functions; the different possible gauges, their advantages and drawbacks; and specificities of the treatment of periodic systems. In line with the well-established generic theorems in DFPT, the second-order derivative of the free energy is formulated as a variational functional of trial first-order wave functions and the trial first-order density matrix. A contribution from the second-order entropy is present in the second-order free energy. The changes of the occupation numbers are explicitly considered.

Concerning applications, this formalism has been available for some time in ABINIT and has already yielded many publications. Nevertheless, two advanced application-related topics have been covered. For the first topic, the study of the convergence of phonon frequencies with respect to wave vector sampling, two regimes, medium and high precision, naturally emerge, corresponding to whether the phonon frequencies or temperature dependence as such are the target property. The second topic relates to the impact of the preliminary unperturbed calculation on the subsequent DFPT calculation if the unoccupied wave functions have not been sufficiently accurately computed.

## ACKNOWLEDGMENTS

This paper was supported by the Fonds de la Recherche Scientifique (FRS-FNRS Belgium) through the PdR Grant No. T.0103.19—ALPS. It is an outcome of the Shapeable 2D Magnetolectronics by Design Project (SHAPEme, EOS Project No. 560400077525) that received funding from the FWO and FRS-FNRS under the Belgian Excellence of

Science (EOS) program. Ch.T. acknowledges support from the Research Council of Norway through its Centres of Excellence scheme (Grant No. 262695), through the FRIPRO grant

ReMRChem (Grant No. 324590), and from NOTUR—The Norwegian Metacenter for Computational Science through a grant of computer time (Grant No. nn14654k).

- 
- [1] S. Baroni, P. Giannozzi, and A. Testa, *Phys. Rev. Lett.* **58**, 1861 (1987).
- [2] X. Gonze, D. C. Allan, and M. P. Teter, *Phys. Rev. Lett.* **68**, 3603 (1992).
- [3] S. de Gironcoli, *Phys. Rev. B* **51**, 6773 (1995).
- [4] X. Gonze, *Phys. Rev. A* **52**, 1096 (1995).
- [5] X. Gonze, *Phys. Rev. B* **55**, 10337 (1997).
- [6] X. Gonze and C. Lee, *Phys. Rev. B* **55**, 10355 (1997).
- [7] S. Baroni, S. de Gironcoli, A. Dal Corso, and P. Giannozzi, *Rev. Mod. Phys.* **73**, 515 (2001).
- [8] X. Gonze, G. M. Rignanese, and R. Caracas, *Z. Kristallogr. Cryst. Mater.* **220**, 458 (2005).
- [9] X. Wu, D. Vanderbilt, and D. R. Hamann, *Phys. Rev. B* **72**, 035105 (2005).
- [10] F. Ricci, S. Prokhorenko, M. Torrent, M. J. Verstraete, and E. Bousquet, *Phys. Rev. B* **99**, 184404 (2019).
- [11] G. Petretto, S. Dwaraknath, H. P. Miranda, D. Winston, M. Giantomassi, M. J. van Setten, X. Gonze, K. A. Persson, G. Hautier, and G.-M. Rignanese, *Sci. Data* **5**, 180065 (2018).
- [12] L. He, F. Liu, G. Hautier, M. J. T. Oliveira, M. A. L. Marques, F. D. Vila, J. J. Rehr, G.-M. Rignanese, and A. Zhou, *Phys. Rev. B* **89**, 064305 (2014).
- [13] P. Ghosez, J. P. Michenaud, and X. Gonze, *Phys. Rev. B* **58**, 6224 (1998).
- [14] A. Fleszar and X. Gonze, *Phys. Rev. Lett.* **64**, 2961 (1990).
- [15] G. M. Rignanese, J. P. Michenaud, and X. Gonze, *Phys. Rev. B* **53**, 4488 (1996).
- [16] M. Veithen, X. Gonze, and Ph. Ghosez, *Phys. Rev. B* **71**, 125107 (2005).
- [17] M. Veithen, X. Gonze, and P. Ghosez, *Phys. Rev. Lett.* **93**, 187401 (2004).
- [18] F. Giustino, *Rev. Mod. Phys.* **89**, 015003 (2017).
- [19] A. Miglio, V. Brousseau-Couture, E. Godbout, G. Antonius, Y.-H. Chan, S. G. Louie, M. Côté, M. Giantomassi, and X. Gonze, *npj Comput. Mater.* **6**, 167 (2020).
- [20] X. Gonze and J. P. Vigneron, *Phys. Rev. B* **39**, 13120 (1989).
- [21] A. Debernardi, *Solid State Commun.* **113**, 1 (1999).
- [22] M. Royo and M. Stengel, *Phys. Rev. X* **9**, 021050 (2019).
- [23] C. Lee and X. Gonze, *Phys. Rev. B* **51**, 8610 (1995).
- [24] X. Gonze, *Phys. Rev. A* **52**, 1086 (1995).
- [25] M. Methfessel and A. T. Paxton, *Phys. Rev. B* **40**, 3616 (1989).
- [26] F. J. dos Santos and N. Marzari, *Phys. Rev. B* **107**, 195122 (2023).
- [27] X. Gonze, J. M. Beuken, R. Caracas, F. Detraux, M. Fuchs, G. M. Rignanese, L. Sindic, M. Verstraete, G. Zerah, F. Jollet *et al.*, *Comput. Mater. Sci.* **25**, 478 (2002).
- [28] X. Gonze, B. Amadon, G. Antonius, F. Arnardi, L. Baguet, J.-M. Beuken, J. Bieder, F. Bottin, J. Bouchet, E. Bousquet *et al.*, *Comput. Phys. Commun.* **248**, 107042 (2020).
- [29] A. H. Romero, D. C. Allan, B. Amadon, G. Antonius, T. Applencourt, L. Baguet, J. Bieder, F. Bottin, J. Bouchet, E. Bousquet *et al.*, *J. Chem. Phys.* **152**, 124102 (2020).
- [30] M. J. Verstraete, M. Torrent, F. Jollet, G. Zerah, and X. Gonze, *Phys. Rev. B* **78**, 045119 (2008).
- [31] L. E. Díaz-Sánchez, A. H. Romero, M. Cardona, R. K. Kremer, and X. Gonze, *Phys. Rev. Lett.* **99**, 165504 (2007).
- [32] L. E. Díaz-Sánchez, A. H. Romero, and X. Gonze, *Phys. Rev. B* **76**, 104302 (2007).
- [33] M. J. Verstraete, *Phys. Rev. Lett.* **104**, 035501 (2010).
- [34] B. Xu and M. J. Verstraete, *Phys. Rev. Lett.* **112**, 196603 (2014).
- [35] B. Xu and M. J. Verstraete, *Phys. Rev. B* **87**, 134302 (2013).
- [36] E. Cancès, M. F. Herbst, G. Kemlin, A. Levitt, and B. Stamm, *Lett. Math. Phys.* **113**, 21 (2023).
- [37] N. Marzari, D. Vanderbilt, and M. C. Payne, *Phys. Rev. Lett.* **79**, 1337 (1997).
- [38] M. Verstraete and X. Gonze, *Phys. Rev. B* **65**, 035111 (2001).
- [39] See Supplemental Material at <http://link.aps.org/supplemental/10.1103/PhysRevB.109.014317> for the content described in several paragraphs of the Introduction.
- [40] N. Marzari, D. Vanderbilt, A. De Vita, and M. C. Payne, *Phys. Rev. Lett.* **82**, 3296 (1999).
- [41] M. Verstraete and X. Gonze, *Comput. Mater. Sci.* **30**, 27 (2004).
- [42] H. Hellmann, *Einführung in die Quantenchemie* (Deuticke, Leipzig, 1937).
- [43] R. P. Feynman, *Phys. Rev.* **56**, 340 (1939).
- [44] D. R. Hamann, *Phys. Rev. B* **88**, 085117 (2013).
- [45] M. van Setten, M. Giantomassi, E. Bousquet, M. Verstraete, D. Hamann, X. Gonze, and G.-M. Rignanese, *Comput. Phys. Commun.* **226**, 39 (2018).